GIS-BASED STATISTICAL ANALYSIS USING FIVE DIFFERENT METHODS FOR LANDSLIDE VULNERABILITY MAPPING AND COMPARISON OF THEIR PERFORMANCE IN KANGRA, HIMACHAL PRADESH, INDIA

A DISSERTATION

SUBMITTED IN PARTIAL FULFILLMENT OF THE REQUIREMENT FOR THE AWARD OF THE DEGREE OF

MASTER OF TECHNOLOGY

IN

GEOTECHNICAL ENGINEERING

Submitted by:

ANSHU KUMAR

(2K21/GTE/06)

Under the Supervision of

PROF. RAJU SARKAR

DEPARTMENT OF CIVIL ENGINEERING

DELHI TECHNOLOGICAL UNIVERSITY

(Formerly Delhi College of Engineering)

Bawana Road, Delhi-110042

MAY 2023

DEPARTMENT OF CIVIL ENGINEERING
DELHI TECHNOLOGICAL UNIVERSITY
(Formerly Delhi College of Engineering)
Bawana Road, Delhi-110042

CANDIDATE'S DECLARATION

I, Anshu Kumar, Roll No – 2K21/GTE/06, a student of M. Tech. in Geotechnical Engineering, declare that the project Dissertation titled "GIS-based statistical analysis using five different methods for landslide vulnerability mapping and comparison of their performance in Kangra, Himachal Pradesh, India" which is submitted by me to the Department of Civil Engineering, Delhi Technological University, Delhi for the partial fulfillment of the requirement for the award of the degree of Master of Technology, is original and not copied from any source without proper citation. This work has not previously formed the basis for the award of any Degree, Diploma Associateship, Fellowship, or other similar title or recognition.

Place: Delhi **ANSHU KUMAR**

Date: 31/05/2023

DELHI TECHNOLOGICAL UNIVERSITY

(Formerly Delhi College of Engineering)

Bawana Road, Delhi-110042

CERTIFICATE

I hereby certify that the Project Dissertation titled “GIS-based statistical analysis using five different methods for landslide vulnerability mapping and comparison of their performance in Kangra, Himachal Pradesh, India” which is submitted by Anshu Kumar; Roll No 2K2/GTE/06; Department of Civil Engineering, Delhi Technological University, Delhi for the partial fulfillment of the requirement for the award of the degree of Master of Technology, is a record of the project work carried out by the student under my supervision. To the best of my knowledge, this work has not been submitted in part or full for any Degree at this University or elsewhere.

Place: Delhi **PROF. RAJU SARKAR**

Date: 31/05/2023 **SUPERVISOR**

Department of Civil Engineering

Delhi Technological University

Bawana Road, Delhi-110042

ABSTRACT

Landslides are among the most devastating elements on the globe, causing many deaths and financial losses every year. The investigation of variables causing the incidence of landslides in an area and the zoning of the consequent damages will undoubtedly play an important role in minimizing such events. Kangra, the district of Himachal Pradesh, India has experienced frequent landslides in the past decades making it important for the study. The landslide vulnerability zonation map has been formulated by applying 5 non - identical statistical models namely, frequency ratio (FR), Shannon's entropy (SE), information value (IV), Weight of evidence (WoE), and certainty factor (CF) models. We have considered a total of 200 landslide points at different locations in Kangra for our research purpose. Landslide inventory is created by dividing the total landslide points into training data (80%) and testing data (20%). There can be a lot of triggering factors for landslides but we have taken 13 factors into consideration namely, elevation, slope, curvature, aspect, SPI, TWI, rainfall, distance to roads, rivers & lineaments, LULC, geology, and lithology. The vulnerability map is then created using the 5 models and a comparison is done between them. Then, the map created by the above-mentioned 5 models is validated with the help of a testing data set using the AUC (Area under curve) of the ROC (Receiver Operating Characteristics) curve. The AUC comes out to be 0.863, 0.844, 0.83, 0.88, and 0.88 for FR, SE, IV, WoE, and CF model respectively. These maps can be further utilized by the government in mitigation planning.

ACKNOWLEDGEMENT

The following research work is the final output of my two years master's degree in Geotechnical Engineering at the Delhi Technological University (DTU), New Delhi, India. I would like to express my heartfelt appreciation to the Delhi Technological University (DTU) staff for their prompt academic and administrative support, without which this work would not have been successful.

I am grateful to my thesis supervisor, **Prof. Raju Sarkar** for his valuable guidance and constructive scholarly suggestions during the planning and implementation of my project work. Without his timely inputs and periodic assessments, this project would not have given the desired results.

I would like to thank **Prof. V K Minocha** (Head of the Department, Delhi technological university) and my teachers for motivating and inspiring me throughout this journey, and for their brilliant comments and suggestions.

I would like to extend my heartfelt appreciation to my family members for their constant encouragement and support for the completion of the course. I would also like to thank my friends in the college throughout the study program with whom I gained valuable experiences through which I tried to dive into the deep sea of knowledge.

ANSHU KUMAR

TABLE OF CONTENTS

LIST OF TABLES

LIST OF FIGURES

CHAPTER 1

INTRODUCTION

1.1. BACKGROUND AND MOTIVATION OF RESEARCH

Landslides are the most prevalent geological calamity, resulting in human deaths and economic damage. Many landslide catastrophes in the Himalayas have recently greatly impacted civilization. Hill slopes are being disturbed as a result of expanding urbanization due to numerous construction operations, including road and building development. It is critical to have a thorough comprehension of the interaction between the propensity and activating elements that activate landslide occurrence in every location. Kangra is one of the famous tourist spots. Landslide vulnerability mappings may be utilized as an efficient technique that can offer further efforts in landslide mitigation. With the upsurge of landslides, a large scale of research work is taking place using GPS, RS, and GIS using different approaches. There are various types of approaches for creating the vulnerability map such as deterministic approach, heuristic approach, and statistical approach. In the heuristic approach, the map is created with expert opinions which can vary from person to person. In the deterministic approach, a lot of data is required based on field investigation for the collection of all the soil data which is not easy to carry for a larger area. In the statistical approach, they incorporate randomness in their approach. The statistical approach is further of two types, bivariate analysis, and multivariate analysis. In a bivariate analysis, two observations from a single sample or person are used to examine the interaction between two data sets. Nevertheless, every sample is not dependent on each other. The multivariate analysis investigates numerous factors to discover if one or more of them are predictive of a given result. The outcome is the dependent variable, while the predictive variables are the not dependent variables. Without validating the models, they will be of no use. Therefore, all the models must be validated to observe their performance of the model. The AUC is mostly used for

calculating the model's accuracy. The success rate curve (SRC) and prediction rate curve (PRC) are plotted using training and testing points.

1.2. AIM OF THE RESEARCH WORK

This research work has been carried out to find a relationship between various approaches used for the preparation of landslide susceptibility mapping of the Kangra district of Himachal Pradesh, India. The dominance of causative factors has also been carried out for the area of research.

The outputs of this research can be used by the government and higher authorities for any type of development project or market, cities, highways, tourist attractions, and so on. These maps will be invaluable to planners and policymakers in developing strategies to limit and save the devastation caused by landslides.

1.3. OBJECTIVES

The objectives of the research can be listed as:

- To create a distinctive thematic map for each landslide activating factor of the study area.
- To prepare Landslide Vulnerability Map using Frequency Ratio, Shannon's Entropy, Information Value, Weigh of Evidence, and Certainty Factor models.
- Validation of models using the Area under the curve (AUC) approach of the Receiver Operating Characteristic (ROC) curve for both the training and testing datasets of landslide inventory for both models.
- Establishing a relationship between the models on the basis of their Success rate curve and Prediction rate curve.
- Calculation of landslide-prone areas using all five models for Kangra.

CHAPTER 2

LITERATURE REVIEW

2.1. LITERATURE WORK

The research work carried out by various researchers is tabulated as shown in Table 2.1. The table includes Author's name, study area, landslide points, activating factors, methods adopted, and their result (Area under the curve).

Table 2.1. Literature survey

	Author's Name	Study Area	Landslide Points	Factors	Methods Adopted	AUC
1	Pasang et al. (2020)	Asian Highway, Bhutan	120	land cover, lithology, elevation, proximity to roads, drainage, fault lines, aspect, and slope angle	WoE, IV, and LR	0.883, 0.882 and 0.88
2	Li et al. (2016)	Daguan County, China	194	slope angle, slope aspect, general curvature, plan curvature, profile curvature, altitude, distance from rivers, distance from roads, distance from faults, lithology, NDVI, STI, SPI, and TWI	EBF and WoE	0.801 and 0.807
3	Cao et al. (2021)	Xunyang District	556	slope angle, aspect, curvature, stratigraphic units, distance to faults, rivers & roads	WoE	0.919
4	Hussain et al. (2019)	National Highway – 1, J&K	60	slope, aspect, curvature, relief, lithology, LULC,	FR and WoE	0.865 and 0.768

				proximity to the river, proximity to the road, and proximity to lineament		
5	Kayasatha (2015)	Garuwa sub-basin, East Nepal	136	slope aspect, slope angle, slope shape, relative relief, geology, distance from faults, land use, distance from drainage, and annual rainfall,	FR	0.811
6	Mersha et al. (2020)	Simada area, northwestern Ethiopia	576	aspect, slope, curvature, lithology, land use, rainfall, and distance to stream	FR and WoE	0.882 and 0.848
7	Regmi et al. (2014)	Mugling–Narayanghat Road section	295	slope gradient, slope aspect, plan curvature, altitude, SPI, TWI, lithology, land use, distance from faults, distance from rivers, and distance from highways	FR, SI, and WoE	0.768, 0.756 and 0.755
8	Sarkar et al. (2013)	Darjeeling Himalayas	51	slope, rainfall, earthquake, lineament density, drainage density, geology, geomorphology, aspect, land use and land cover, and soil	IV	0.890
9	Razavizade et al. (2017)	Mazandaran Province, Iran	105	slope degree, slope aspect, altitude, plan curvature, SPI, TWI, STI, TRI, lithology, distance from streams, faults, roads, and land use type	FR, WoE, and SI	0.815, 0.794 and 0.812
10	Yilmaz (2009)	Kat County (Tokat—Turkey)	57	geology, faults, drainage system, topographical elevation, slope	FR, LR, and ANN	0.826, 0.842 and 0.852

				angle, slope aspect, TWI, and SPI		
11	Chen et al. (2016)	Shangzhou District of Shangluo City, China	145	slope aspect, curvature, slope angle, elevation, distance to rivers, distance to faults, lithology, peak ground acceleration, distance to roads, and precipitation	FR and WoE	0.763 and 0.745
12	Dam et al. (2022)	Pithoragarh district of Uttarakhand	91	slope degree, aspect, curvature, elevation, land cover, slope forming materials, geomorphology, distance to rivers, distance to roads, and overburden depth	SE and WOE	0.521 and 0.687
13	Poudyal et al. (2010)	Panchthar District, Nepal	111	slope angle, aspect, curvature land use, SPI, TWI, LS, Lithology, Distance from drainage & lineaments	FR and ANN	0.822 and 0.782
14	Sharma et al. (2019)	Himalayan watershed	190	slope, aspect, lithology, curvature, lineament density, land cover, and drainage buffer	FR, AHP, and IV	0.896, 0.871 and 0.882
15	Mondal et al. (2019)	Darjeeling Himalaya	2079	elevation, aspect, slope, curvature, geology, soil, lineament density, distance to lineament, DD, distance to drainage, SPI, TWI, rainfall, NDVI, and LULC	IOE	0.782
16	Gautam et al. (2021)	Indrawati watershed, Nepal	264	slope, aspect, elevation, geological formation, proximity to the river, proximity to	FR, LR, ANN, SVM	0.801, 0.856, 0.869 and 0.869

				the road, land cover, soil type, and curvature		
17	Alsabhan et al. (2022)	Himachal Pradesh	123	aspect, curvature, elevation, LULC, soil, lithology, and drainage density	WOE, FR, and IVM	0.762, 0.7820 and 0.76
18	Du et al. (2019)	Eastern Himalayan syntaxis in Tibet	799	lithology, slope gradient, slope aspect, elevation, curvature, distance to faults, distance to drainages, and distance to roads	AHPIV and LRIV	0.884 and 0.906
19	Wu et al. (2017)	Daguan County, Yunnan Province, China	136	slope angle, slope aspect, curvature, plan curvature, profile curvature, altitude, STI, SPI, TWI, NDVI, rainfall, distance to faults, distance to roads, and distance to the lithology	LR and SI	0.802 and 0.810
20	Chen et al. (2017)	Qianyang County of Baoji City, China	81	angle of slope, slope aspect, curvature, plan curvature, profile curvature, altitude, distance to faults, distance to rivers, distance to roads, STI, SPI, TWI, and lithology	FR, SI, and WoE	0.8362, 0.8345 and 08251
21	Kumar et al. (2021)	Goriganga Valley, Kumaun Himalaya	421	lithology, slope angle, slope aspect, elevation, curvature plan, curvature profile, distance to drainage, road & thrusts, land use, and land cover, rainfall and peak ground acceleration	YC, FR, InV, WoE and ANN	Between 0.84 to 0.86 and ANN 0.904
22	Demir et al. (2015)	North Anatolian Fault Zone in Tokat province	251	elevation, slope gradient, slope aspect, distance to streams, roads, faults, drainage	LR and FR	0.708 and 0.744

				density, and fault density		
23	Chen et al. (2016)	Baozhong region of Baoji City, China	79	slope degree, slope aspect, plan curvature, altitude, geomorphology, lithology, distance from faults, distance from rivers, and precipitation	AHP and CF	0.759 and 0.814
24	Park et al. (2013)	Republic of Korea	708	elevation, slope, aspect, distance to drainage, SPI, TWI, soil texture, soil effective thickness, tree type, tree diameter, tree age, crown density, land use/land cover type	FR, AHP, LR, and ANN	0.794, 0.789, 0.794, and 0.806
25	Sameen et al. (2020)	Chukha Dzongkhag, Bhutan	952	altitude, slope, aspect, curvature, slope length, TWI, STI, lithology, nearness to roads & streams	SAE-RGF, RGF, RF	0.931, 0.972 and 0.824

2.2. LITERATURE GAPS

Not a lot of research has been carried out for the preparation of landslide vulnerability mapping in the Kangra district of Himachal Pradesh.

Although the use of statistical bivariate approaches for landslip susceptibility mapping has received substantial attention recently, particularly with the introduction of cutting-edge technology and methodology, there remains a significant publication void in this area.

The corpus of research already done on landslip susceptibility mapping uses a variety of methodologies, such as statistical, machine learning, and hybrid methods. In order to determine landslip susceptibility, these techniques frequently concentrate on multivariate studies, combining several environmental and topographic aspects. Comprehensive

research that investigates the particular use of statistical bivariate approaches for this goal is lacking, nonetheless.

Numerous disciplines, including ecology, hydrology, and geology, have shown the value of statistical bivariate approaches, which generally analyze two variables. Their potential for landslide susceptibility mapping hasn't been fully realized, though. Insights into the connections between certain factors and landslide occurrences may be gained through the use of bivariate approaches, which improve evaluations of susceptibility and our knowledge of the underlying processes.

A total of 5 GIS-based statistical bivariate methods i.e., Frequency Ratio, Shannon's Entropy, Information Value, Weight of Evidence, and Certainty factor methods are used which was not done earlier.

2.3. LANDSLIDE DEFINITION AND TYPES

Landslide refers to a broad range of mechanisms that cause slope-forming materials, such as rock, soil, artificial fill, or a mix of these, to move outward and downward. It's possible for the materials to move via toppling, sliding, spreading, or flowing.

Table 2.2. Classification of Landslides

TYPE OF MOVEMENT		**TYPE OF MATERIAL**		
		BED ROCK	**ENGINEERING SOILS**	
			Predominantly coarse	Predominantly fine
FALLS		Rock fall	Debris fall	Earth fall
TOPPLES		Rock topple	Debris topple	Earth topple
SLIDES	**ROTATIONAL**	Rock slide	Debris slide	Earth slide
	TRANSLATIONAL			
LATERAL SPREAD		Rock spread	Debris spread	Earth slide
FLOWS		Rock flow (Deep creep)	Debris flow (Soil creep)	Earth flow (Soil creep)
COMPLEX		Combination of two or more principal types of movement		

Despite being generally associated with hilly locations, landslides may also happen in places with little relief. Landslides can take many different forms in low-relief locations, including cut-and-fill failures (roadway and construction excavations), river bluff failures, lateral spreading landslides, the collapse of mine-waste piles (particularly coal), and a variety of slope failures connected to quarries and open pit mines [27], [16]. The classification of landslides is shown in Table 2.2.

The types of landslides defined by [16] are shown in Fig. 2.1.

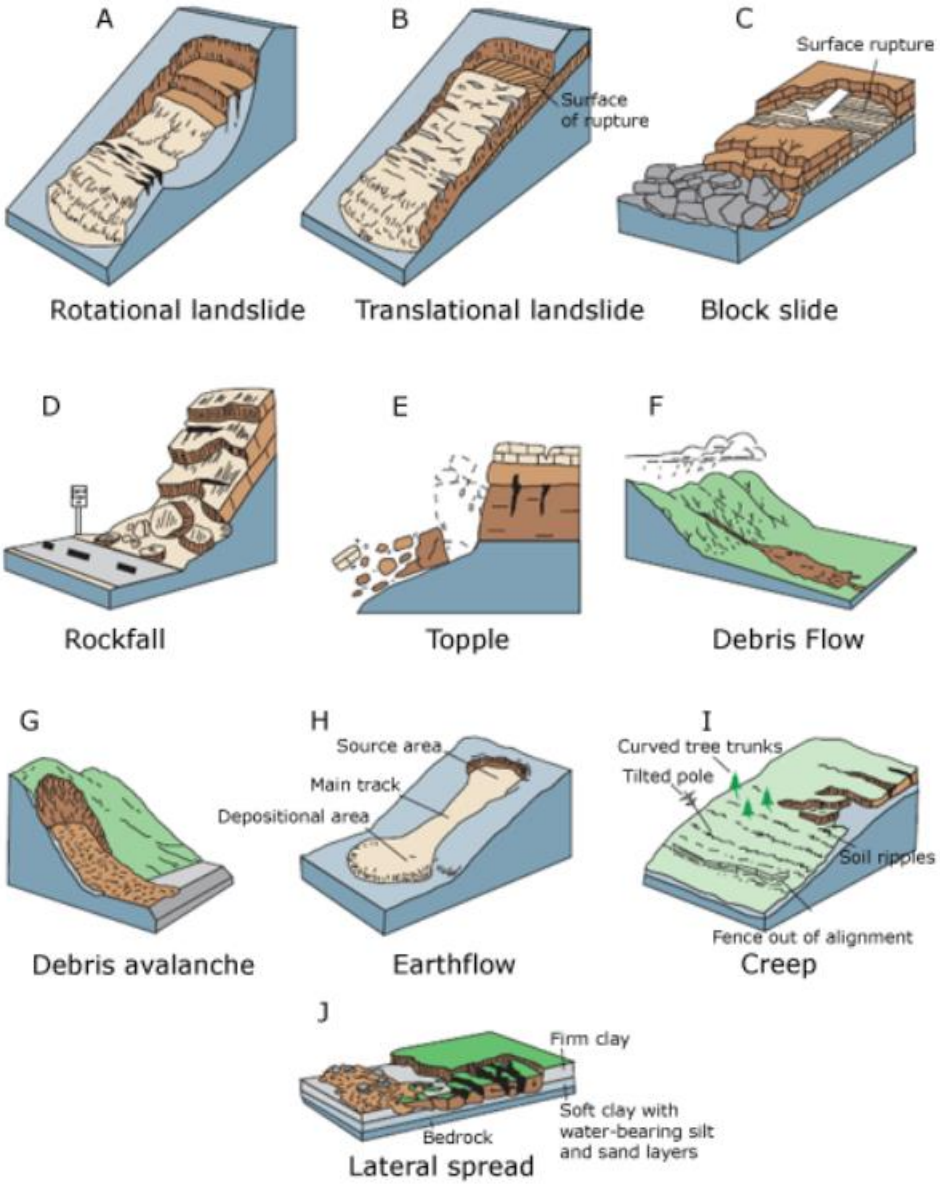

Fig. 2.1. Major types of landslide movements

2.4. REMOTE SENSING AND GEOGRAPHIC INFORMATION SYSTEM

Due to the spatial, spectral, temporal, and radiometric resolutions at which sensor systems and reconnaissance platforms operate, remote sensing (RS) offers a method for evaluating the terrain. Temporal resolution is the periodicity or return interval of a satellite within its designated orbit around the Earth. Radiometric resolution is the range of intensity levels used to quantify spectral responses evaluated by the respective sensor system. Spatial resolution refers to the ground area simultaneously (Instantaneous Field of View) sensed by a particular sensor system [6], [10].

Using a radiance-intensity range design to distinguish between landscape features and process variables, the four remote sensing resolutions work together to characterize the landscape at local, regional, seasonal, annual, and global spatial scales. Additionally, satellites provide a viewpoint on Earth observation, computer compatibility of sensed data, historical views, and almost worldwide coverage for landscape research [9].

Geographic Information System (GIS) technology combines a system capable of data capture, storage, administration, retrieval, analysis, and presentation to give an analytical framework for data synthesis [32], [23]. From a functional standpoint, GIS methods exhibit the following traits:

1. Spatial and non-spatial relationship
2. Representation of landscape perspective
3. Display of information for spatial and temporal pattern
4. Co-occurrence of spatial and non-spatial data
5. Display of thematic coverage
6. Modelling of location and response of phenomena

2.5. LANDSLIDE VULNERABILITY MAPPING

The method of mapping landslide susceptibility involves determining which places are vulnerable to landslides based on a range of variables, including terrain, geology, rainfall patterns, land use, and human activities [14]. By supplying information to decision-

makers, such mapping aims to lower the danger of landslides and the effects they have on people, property, and infrastructure [25], [26], [34].

The following phases are commonly included in the mapping of the landslide susceptibility process:

- Data gathering: This entails compiling details on the topography, geology, soil properties, land usage, and other elements that may have an impact on landslip susceptibility.
- Identifying places that are vulnerable to landslides based on the existence of triggering variables including steep slopes, unstable soils, and excessive rainfall is known as hazard assessment.
- Analysis of the population and infrastructure in the indicated danger zones' exposure, sensitivity, and capability for adaptation constitutes vulnerability assessment.
- Risk assessment: This process combines vulnerability and hazard analyses to pinpoint the most vulnerable places to landslides.
- Making maps that depict the various degrees of landslip susceptibility in the studied region is known as mapping.
- Communication and planning: This requires informing decision-makers and stakeholders of the findings of the landslide vulnerability mapping and devising plans and strategies to lower the risk of landslides in the designated hazard zones.

In general, landslide vulnerability mapping is a crucial tool for risk reduction and disaster management because it enables decision-makers to pinpoint locations that are most at risk for landslides and to take the necessary precautions to lessen both the likelihood of their occurring and their effects.

2.6. METHODS OF PREPARATION OF VULNERABILITY MAP

There are various types of approaches for creating the vulnerability map such as deterministic approach, heuristic approach, and statistical approach [7]. In the heuristic approach, the map is created with expert opinions which can vary from person to person. In the deterministic approach, a lot of data is required based on field investigation for the

collection of all the soil data which is not easy to carry for a larger area. In the statistical approach, they incorporate randomness in their approach [22], [2]. The statistical approach is further of two types, bivariate analysis, and multivariate analysis [12]. In a bivariate analysis, two observations from a single sample or person are used to examine the interaction between two data sets [29]. Nevertheless, every sample is not dependent on each other. The multivariate analysis investigates numerous factors to discover if one or more of them are predictive of a given result [28], [18], [24]. The outcome is the dependent variable, while the predictive variables are the not dependent variables. The flowchart showing various approaches used for the preparation of landslide susceptibility/vulnerability mapping is shown in Fig. 2.2.

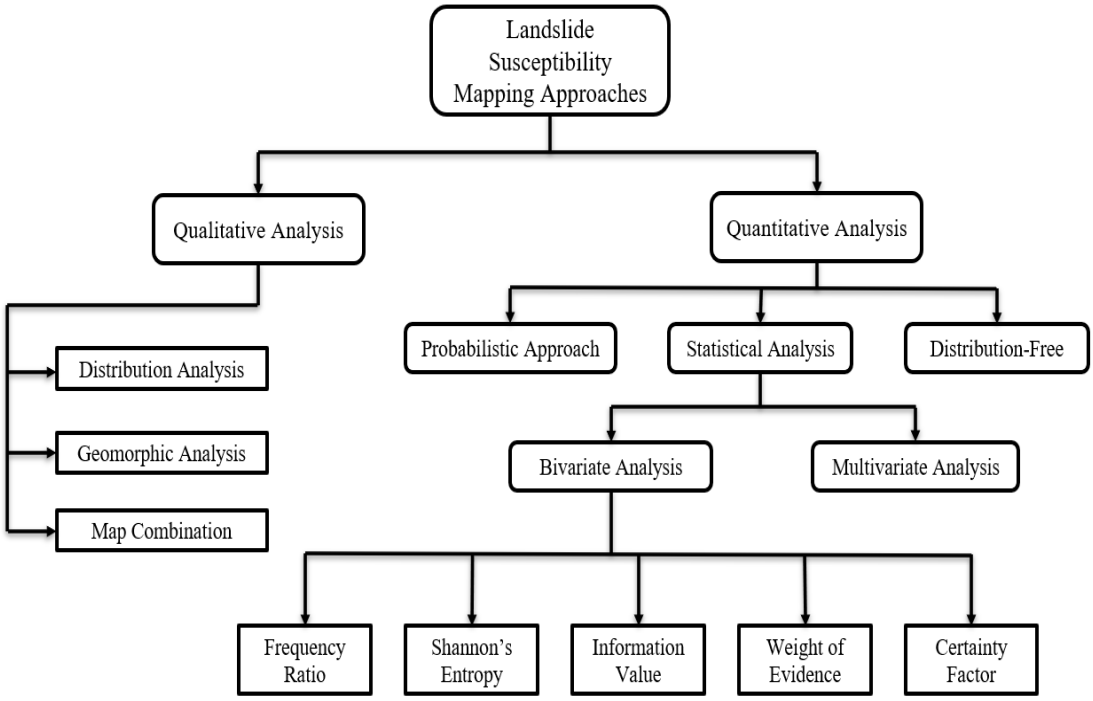

Fig. 2.2. Flowchart showing different approaches for preparation Landslide Susceptibility Mapping

CHAPTER 3

STUDY AREA

3.1. HIMACHAL PRADESH

Himachal Pradesh is a state in the Himalayas in northern India. It is home to resorts like Dalhousie and picturesque mountain villages. Himachal Pradesh, which hosts the Dalai Lama, has a sizable Tibetan population. Its colorful Tibetan New Year celebrations and Buddhist temples and monasteries also reflect this. The area is renowned for its regions for trekking, climbing, and skiing.

According to statistics gathered by the disaster management department, the number of large landslides in Himachal Pradesh increased by a factor of six over the course of the last two years, with 117 happening in 2022 as opposed to 16 in 2020. In the state, there are 17,120 landslide-prone locations, 675 of which are close to vital infrastructure and habitations. Out of the 117 major landslides that were observed in 2022, Kullu reported the most, at 21, followed by Mandi at 20, Lahaul and Spiti at 18, Shimla at 15, Lahaul and Spiti at 14, Sirmaur at 9, Bilaspur at 8, Kangra at 5, Kinnaur at 3, Solan at 1, and Una at 1, but not Hamirpur (outlookindia.com).

All 12 of Himachal's districts are prone to landslides, according to the National Remote Sensing Center's Landslide Atlas of India.

3.2. KANGRA

The Kangra district is located between latitudes 31°21′ and 32°59′ N and longitudes 75°47′55″ and 77°45′ E. It is located on the Himalayas' southern escarpment. The Shivaliks, Dhauladhar, and Himalayas, which range in altitude from northwest to southeast, cut through the entire district. It is bordered on the north by the Punjabi districts of Gurdaspur and Chamba, on the south by Hamirpur and Una, on the east by Mandi, and

on the west by the districts of Chamba and Lahaul and Spiti. The total area is about 5,739 square kilometers, with 3906 villages, 1 municipal corporation, 7 towns, 19 blocks, 14 sub-divisions, and a population of about 15,10,075. The district has a maximum temperature of around 38 degrees in the month of June and a minimum of around 0 degrees in the month of January. Tourists around the globe come to see various places in Kangra such as Masroor temple, Triund, Palampur tea garden, Mcleodganj, Pong-Dam, Kangra fort, Dal Lake, and many more. Fig. 3.1. shows the study area (Kangra district of Himachal Pradesh, Himachal Pradesh and India).

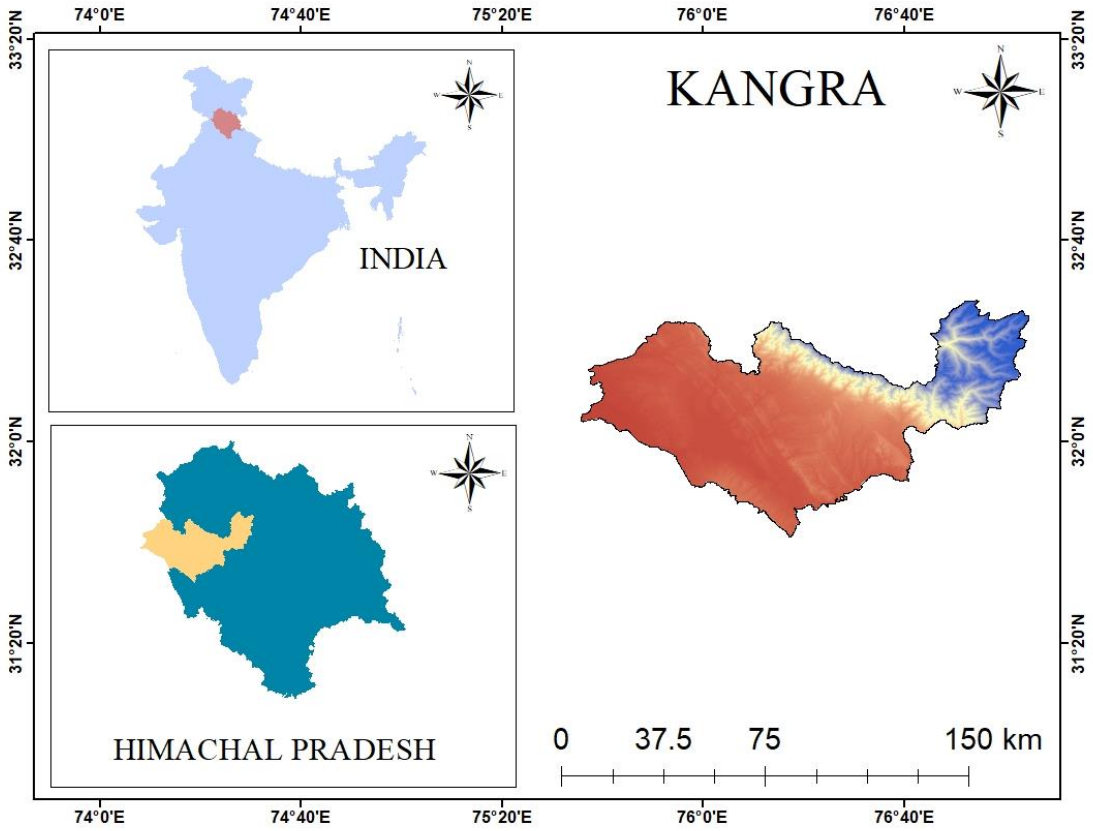

Fig. 3.1. Study area map showing Kangra, Himachal Pradesh and India

CHAPTER 4

METHODOLOGY

4.1. METHODOLOGY ADOPTED

A landslide vulnerability zonation map was created using 5 different models and 13 factors. A landslide vulnerability map detects landslide-prone locations and ranks them from very low to very high. The landslide vulnerability map considers where landslides occur and what is the reason behind them. Our vulnerability map is categorized into 5 classes using the natural break in ArcGIS namely, very low, low, moderate, high, and very high.

After the preparation of the vulnerability map, it is very essential to validate it. For validation purposes, we are using the AUC method of ROC. The SRC and PRC are calculated for every model.

The flow representing the study methodology is shown in Fig. 4.1.

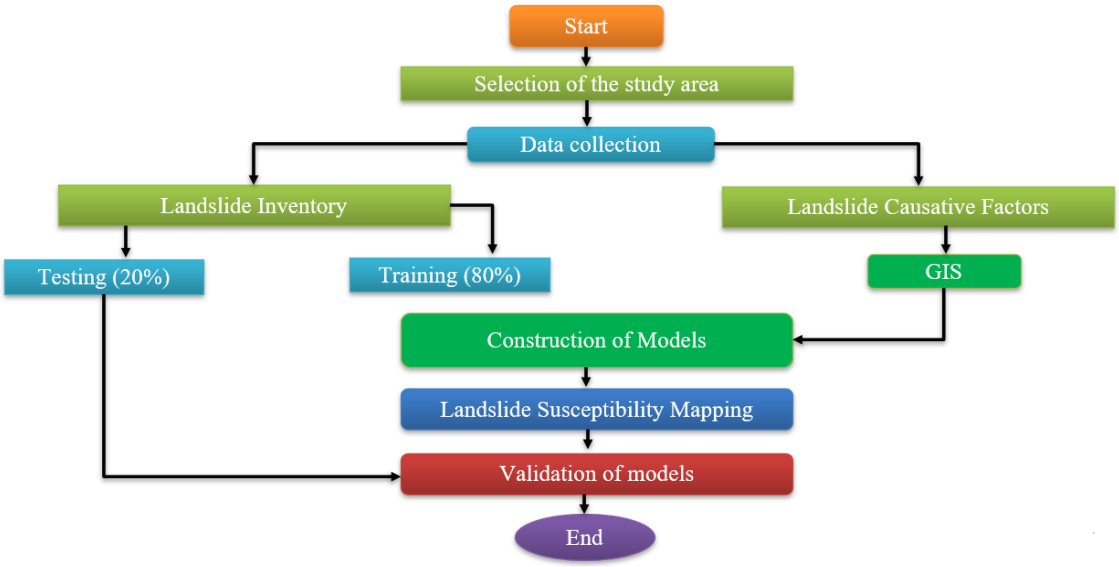

Fig. 4.1. Flow chart of adopted methods

4.2. DATA SOURCES

The data has been collected from various sources in different formats. The digital elevation map was downloaded from Open Topography; SRTM GL1 Global in raster format and the cell size was set to 30m * 30m. The Indian district shapefile was collected from Advances in Geographical Research. The landslide points, distance to roads, rivers & lineaments, geology, and lithology was taken from the Bhukosh portal, GSI. The distance to road, river & lineaments data were in polyline format while the geology and lithology data were in polygon format. The landslide data were in point format. The annual average rainfall data were gathered from Climate Research Unit in the grided format from the year 2011 - 2020. The land use and land cover data were taken from ESRI land cover in raster format. The cell size of all the maps was set to 30m*30m. WGS 1984 UTM Zone 43N projection is used for all maps. A flat, 2D representation of the Earth is a projected coordinate system. Although it is based on a sphere, computations for distance and area are straightforward since the coordinates use linear units of measurement.

4.3. LANDSLIDE CAUSATIVE FACTORS

Since there are too many factors that can cause a landslide, it is not simple to analyze all the factors. So, we have considered 13 factors that lead to the landslide. Elevation, slope, curvature, aspect, SPI, TWI, rainfall, distance to roads, rivers & lineaments, land use land cover, geology, and lithology. Elevation, slope, curvature, aspect, SPI, and TWI are the derivatives of the DEM (Digital Elevation Map) file. They are derived in ArcGIS using tools and some formulations.

4.3.1. Elevation

The elevation can be drawn from the DEM shapefile and then it is masked for the Solan district. The thematic elevation map is constituted of 5 classes. The lowest point is at approximately 196 m whereas the highest point is at 6093 m. The Elevation map is shown in Fig. 4.2.

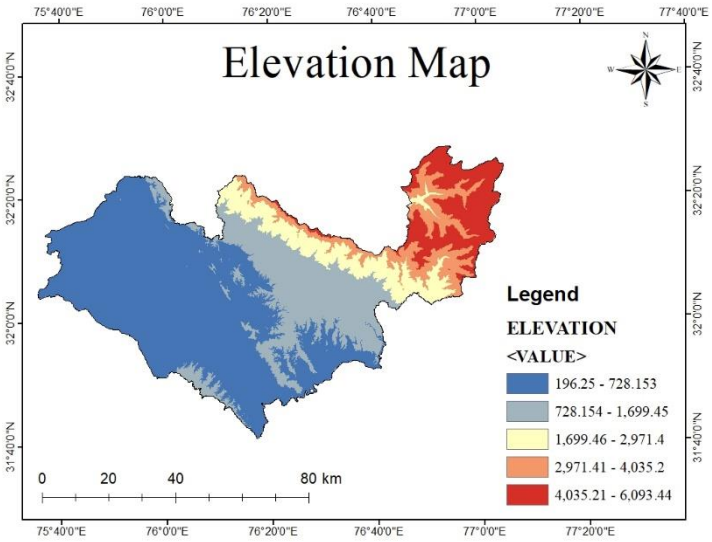

Fig. 4.2. Elevation map

4.3.2. Slope

The slope is the primary determinant of whether landslides will occur. Generally, landslides occur where the value of the slope is very high. It can be said that the higher the value of the slope, the greater will be the probability of the occurrence of a landslide event which establishes a direct interrelationship between them. The map can be derived from the DEM shapefile. The slope map is separated into five sections, with 0 degrees representing the lowest slope and 76 degrees representing the maximum slope. The Slope map is shown in Fig. 4.3.

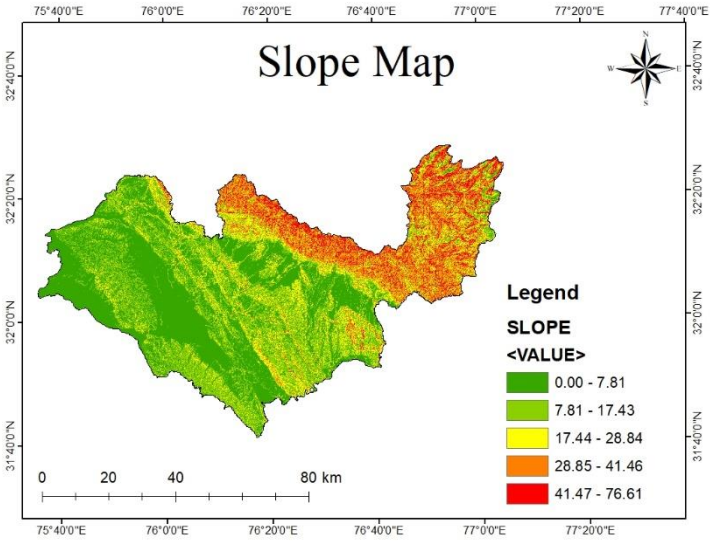

Fig. 4.3. Slope map

4.3.3. Curvature

The curvature represents the shape of the slope. It can also be obtained from the DEM. It is categorized into 5 classes, with (-40.44) being the lowest and 67.33 being the highest value. Convex surfaces are denoted by positive values, concave surfaces are denoted by negative values and flat surfaces are denoted by zero. The Curvature map is shown in Fig. 4.4.

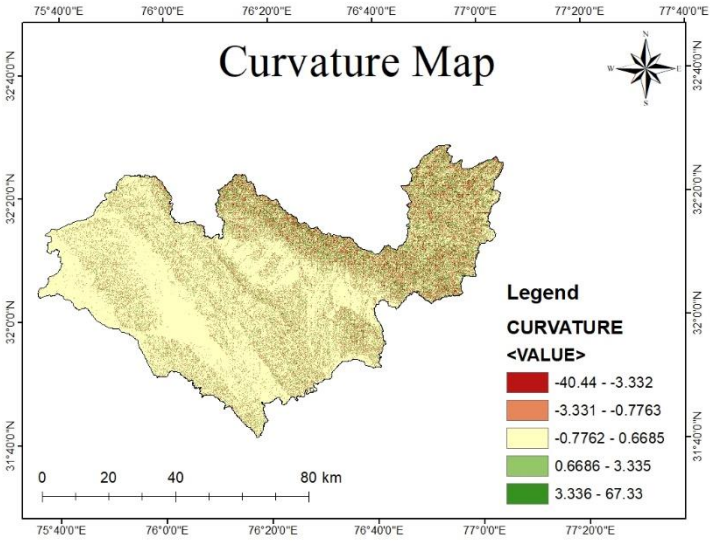

Fig. 4.4. Curvature map

4.3.4. Aspect

It is the portrayal of the slope's direction. It is a derivation of DEM using the spatial analyst tool. Ten classifications are assigned to the aspect starting from (-1) to 360 degrees. The negative value here represents the absence of an aspect. Further, the sections are Flat, North, Northeast, East, Southeast, South, Southwest, West, Northwest, and North as (-1), (0-22.5), (22.5-67.5), (67.5-112.5), (112.5-157.5), (157.5-202.5), (202.5-247.5), (247.5 – 292.5), (292.5-337.5), and (337.5-360) respectively. The Aspect map is shown in Fig. 4.5.

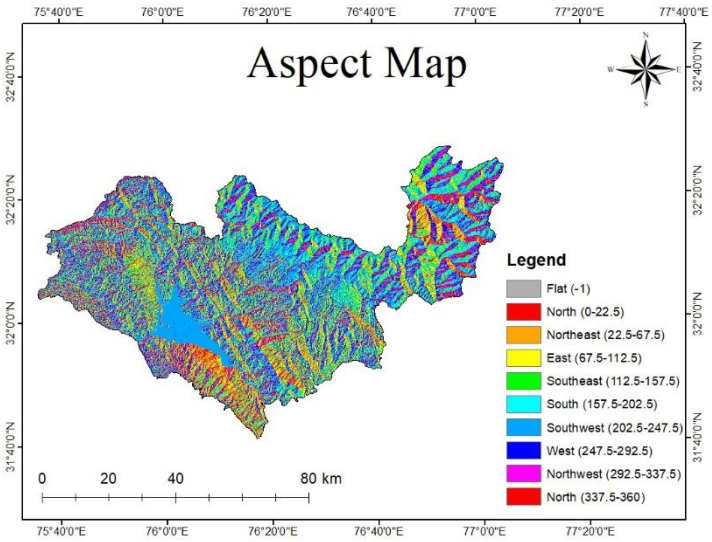

Fig. 4.5. Aspect map

4.3.5. Stream Power Index

The erosive force of water which is in motion is quantified by the SPI. The calculation of SPI is done using slope and area and it approximates the spots on the landscape where gullies are most prone to occur. It can be calculated using the DEM shapefile. SPI is divided into 5 groups with values between (-13.82) and 13.76. The SPI map is shown in Fig. 4.6.

$$SPI = \ln(\text{Flow Accumulation} + 0.001) * ((\text{Slope}(\%)/100) + 0.001) \quad (4.1)$$

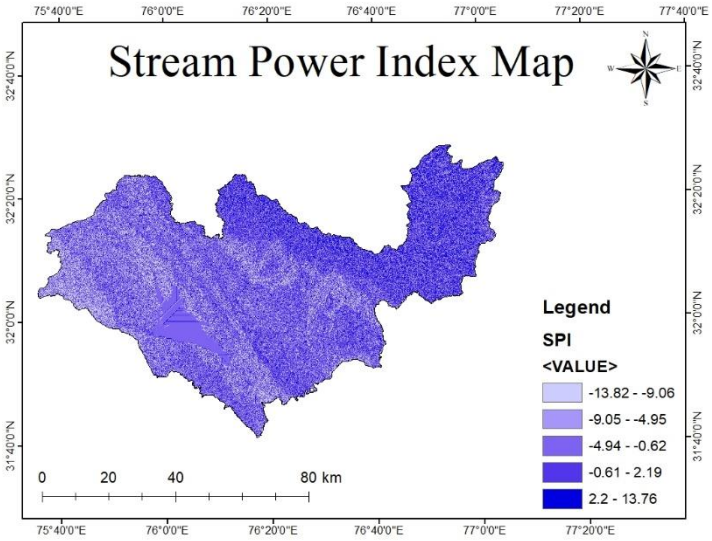

Fig. 4.6. Stream Power Index Map

4.3.6. Topographic Wetness Index

The TWI is created to assess the influences of geographical characteristics on the hydrology procedure. It may be used for a wide range of biological processes, such as the quality of a forest site, the composition of the vegetation, and yearly net primary production. It can be classified into 5 classes ranging from (-8.28) to 21.67. This can also be calculated using DEM. The TWI map is shown in Fig. 4.7.

TWI = ln (Flow Accumulation + 0.001) / ((Slope (%) /100) + 0.001)) (4.2)

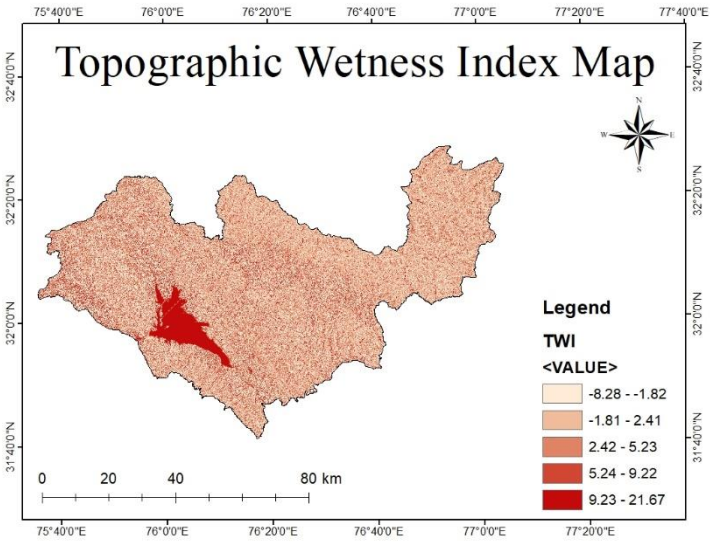

Fig. 4.7. Topographic Wetness Index Map

4.3.7. Rainfall

Rainfall has a big impact on how often landslides happen. It destabilizes the slope. With continuous rainfall, the shear strength decreases because pore water pressure rises, lowering the effective stress. The rainfall data are collected from Climate Research Unit for the last 10 years (2011-2020) in the grided format. And with the help of that data, the Annual average rainfall is calculated using the IDW interpolation tool. The rainfall data are separated into 5 classes, from 670 mm to 1037 mm per year. The rainfall map is shown in Fig. 4.8.

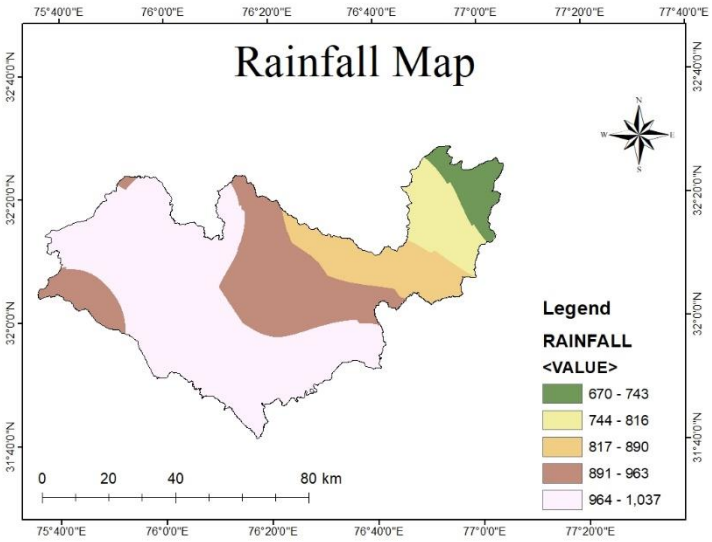

Fig. 4.8. Rainfall Map

4.3.8. Distance to roads

The road is a crucial element in a landslide's likelihood. Roads are built by cutting into the slopes of steep places. Because of the cutting of slopes, the ground becomes unstable, considerably increasing the probability of a landslide. Moreover, research has also revealed that the bulk of the landslides occurs close to the highways. This data is gathered from the Bhukosh Portal, GSI, and with the help of Euclidean Distance, the distance to roads is estimated. The road map's distance is separated into 5 classes, with values ranging from 0 to 14,026 meters. The distance to roads map is shown in Fig. 4.9.

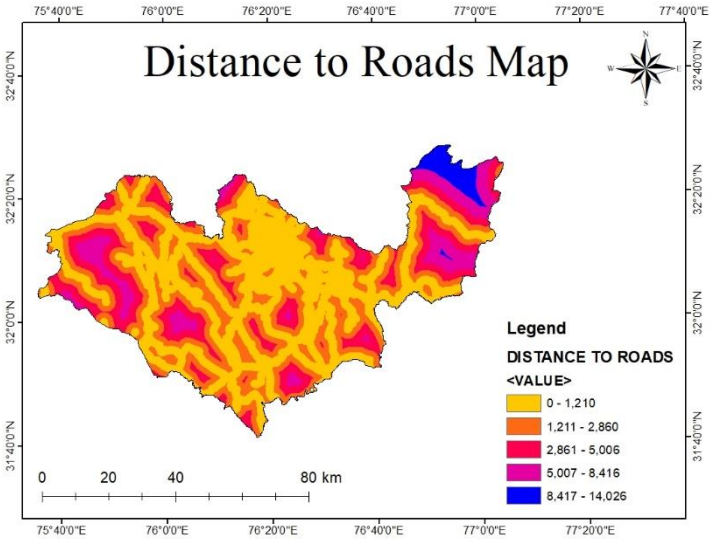

Fig. 4.9. Distance to roads map

4.3.9. Distance to rivers

The presence of rivers disrupts the stability of the slope. Erosion takes place due to the flowing water of the river which weakens the base of the slope and makes it more prone to landslides. The river data is gathered from the Bhukosh portal, GSI, and with the help of the Euclidean Distance, the distance to rivers is calculated. The river map's distance is separated into 5 classes, with values starting from 0 to 54,195 meters. The distance to rivers map is shown in Fig. 4.10.

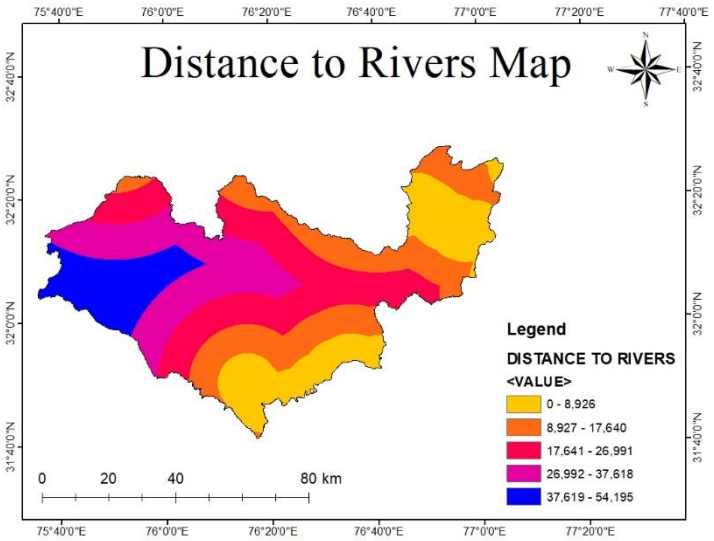

Fig. 4.10. Distance to rivers map

4.3.10. Distance to lineaments

The stability of the slopes is more strongly influenced by geological features such as faults, folds, joints, bedding, and zones of shear. With the increase in faults or lineaments, the area becomes more vulnerable to landslides and earthquakes. The distance to the lineaments is calculated using the Euclidean Distance tool after the lineament data is gathered from Bhukosh, GSI. Lineaments' distance is divided into 5 categories, with distances ranging from 0 to 11,260 meters. The distance to lineaments map is shown in Fig. 4.11.

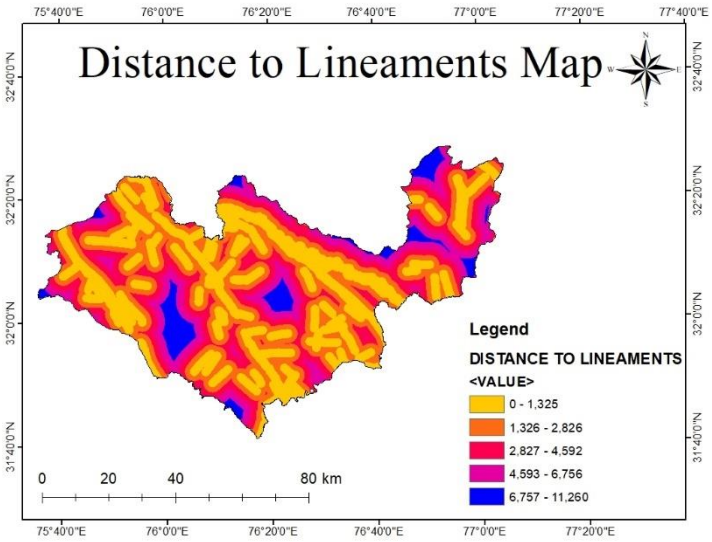

Fig. 4.11. Distance to lineaments map

4.3.11. Land use and Land cover

Changes in land use and land cover can make slopes more susceptible to landslides by affecting the balance between the pressures that keep the soil in place and the forces that cause it to move. As a result, it is essential to examine the influence of human activities on the landscape and to put suitable safeguards in place to limit the danger of landslides in regions where such activities occur. The land use and land cover map is shown in Fig. 4.12.

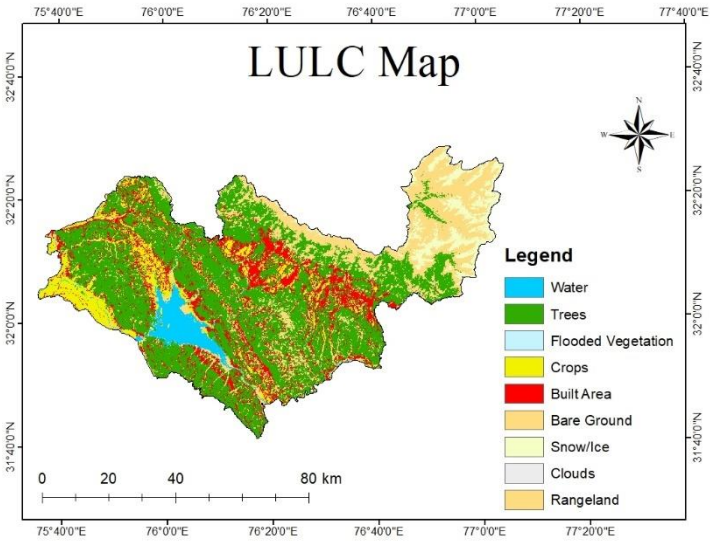

Fig. 4.12. Land use land cover map

4.3.12. Geology

The processes that have shaped the Earth's structure both above and below the surface are explained by geology. It also provides tools for determining the absolute and relative ages of rocks discovered in a certain location as well as for describing the histories of those rocks. The data of Geology is extracted from the Bhukosh Portal. The data is in Raster form which was masked for the study area. Quaternary, Pleistocene, Proterozoic, Pliocene, Miocene, Paleozoic, Neoproterozoic, and Paleoproterozoic are the categories into which geology is separated. The geology map is shown in Fig. 4.13.

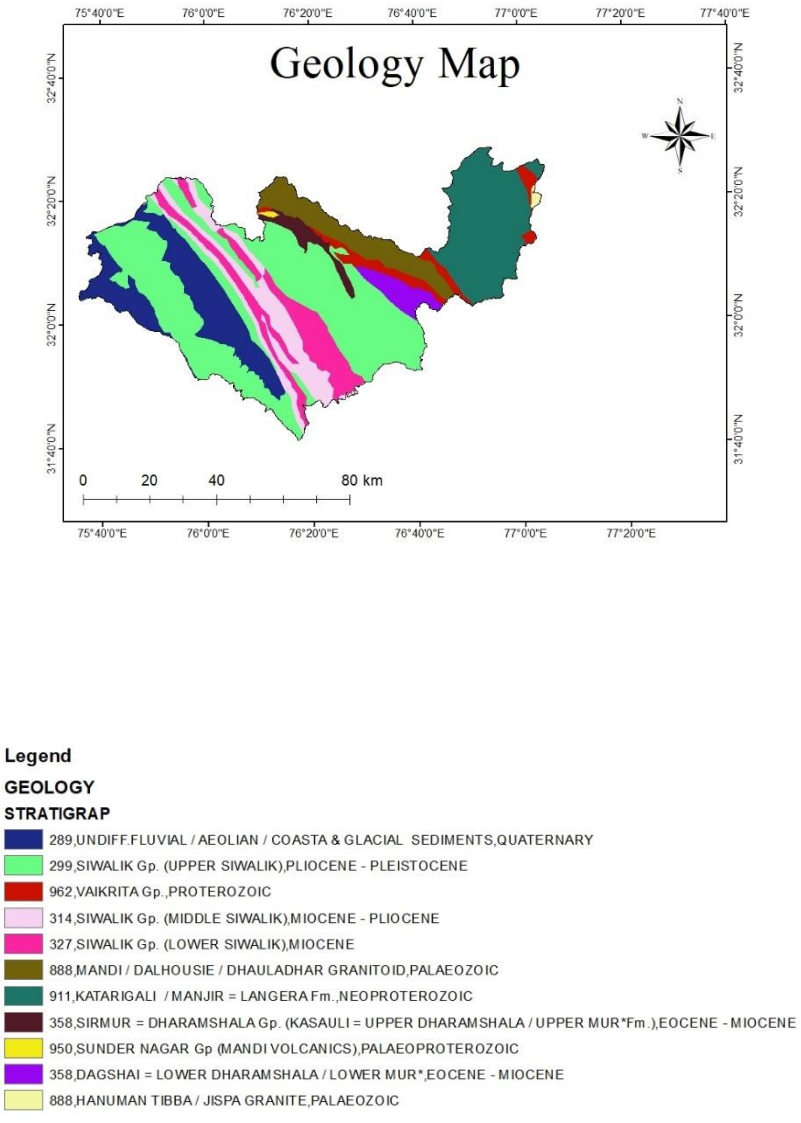

Fig. 4.13. Geology map

4.3.13. Lithology

The kind of rock or soil that makes up a certain location, known as lithology, can have a significant impact on the incidence and features of landslides. Because of their physical and mechanical qualities, some lithologies are more prone to landslides than others. The lithology's unique properties can also influence the type and intensity of landslide that happens. There are a total of 30 lithological formations in the study area. The lithology map is shown in Fig. 4.14.

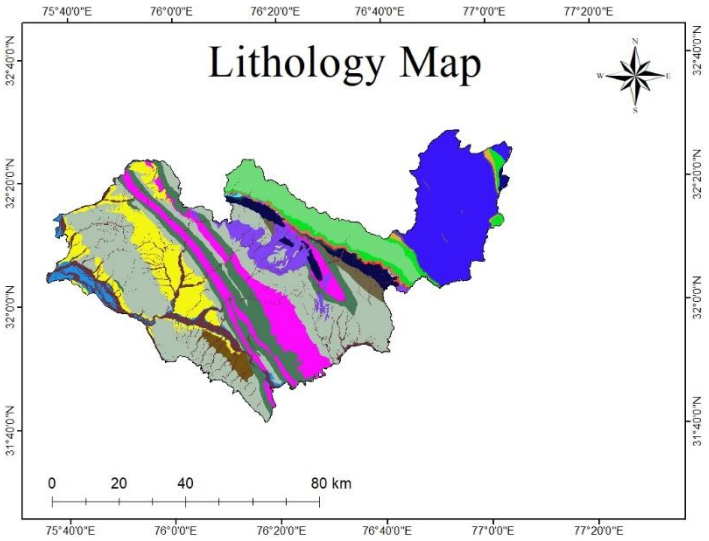

Fig. 4.14. Lithology map

4.4. LANDSLIDE INVENTORY

A landslide inventory map documents the location when the landslide took place and categories of mass movements that have etched discernible marks in a given area. It is the most important part of the creation of the vulnerability map [20]. In our research, we have considered 200 landslide points. These points are split into the training and testing points. In various papers, it was divided as 70 % of the data as training data and 30% as testing data. But, in our case, we have taken 80% of the total points as the training data and 20%

as the testing data. Thus, 160 points (80%) are used as training points and 40 points (20%) are used as testing points. The splitting was done randomly using the subset feature of ArcGIS. The training data is used to form the thematic maps of various factors and the testing data was used last for validation purposes. The landslide inventory is shown in Fig. 4.15.

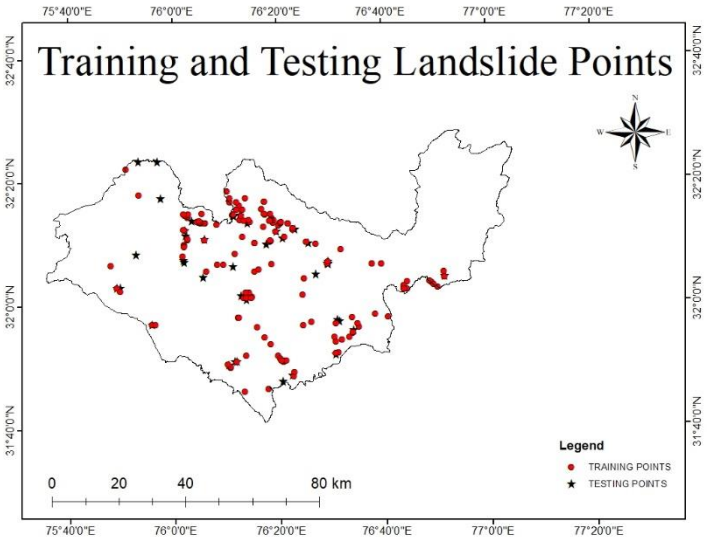

Fig. 4.15. Testing and Training landslide points (Landslide inventory)

CHAPTER 5

MODELS USED

5.1. FREQUENCY RATIO

A FR method is a statistical tool employed in the mapping of landslide vulnerability [8]. It entails determining the link between landslide frequency and numerous activating factors [35], [21], [33]. The prediction rate is calculated with data on the landslide pixel and class pixel. For the calculation of the prediction rate, firstly FR and reduced factor are calculated by equations 5.1 and 5.2. Then, the maps are reclassified on the values of reduced factor as obtained in MS Excel.

$$FR = \frac{\%\ \text{Pixel of landslide}}{\%\ \text{Pixel of class}} \qquad (5.1)$$

$$RF = \frac{FR}{\sum FR\ (\text{for that causative factor})} \qquad (5.2)$$

$$PR = \frac{RFmax - RF\ min}{(RFmax - RF\ min)min} \qquad (5.3)$$

where,

RF = Reduced factor; FR = Frequency Ratio; PR = Prediction Rate

The value of FR above 0 represents a greater likelihood of an event whereas the value of FR below 0 represents a lower likelihood of the event of a landslide.

After calculating the prediction rate, the raster calculator is used to add all the activating factors with their prediction rate. It can be calculated as shown in equation 5.4.

$$LSM = \sum (\text{Prediction Rate} * FR_{maps}) \qquad (5.4)$$

The computational result for the Frequency Ratio for all the factors is shown in Table 5.1.

Table 5.1. Result of Frequency Ratio for every activating factor

CAUSATIVE FACTOR	FACTOR CLASS	LANDSLIDE PIXEL	CLASS PIXEL	FR	RF
ELEVATION (m)	196.25 - 728.15	72900	3356379	0.999	0.274
	728.15 - 1699.45	57600	1343257	1.973	0.542
	1699.46 - 2971.4	8100	555447	0.671	0.184
	2971.4 - 4035.2	0	514361	0.000	0.000
	4035.2 - 6093.44	0	607021	0.000	0.000
		138600	6376465	3.643	1.000

CAUSATIVE FACTOR	FACTOR CLASS	LANDSLIDE PIXEL	CLASS PIXEL	FR	RF
SLOPE (degree)	0 - 7.81	9900	2462173	0.184	0.032
	7.81 - 17.43	40500	1634076	1.137	0.198
	17.44 - 28.84	63000	1006603	2.872	0.500
	28.85 - 41.46	22500	807769	1.278	0.222
	41.47 - 76.61	2700	448659	0.276	0.048
		138600	6359280	5.747	1.000

CAUSATIVE FACTOR	FACTOR CLASS	LANDSLIDE PIXEL	CLASS PIXEL	FR	RF
CURVATURE	(-40.44) - (-3.33)	0	150618	0.000	0.000
	(-3.33) - (-0.77)	23400	978213	1.101	0.264
	(-0.77) - 0.66	79200	4126175	0.883	0.212
	0.66 - 3.33	34200	976437	1.611	0.387
	3.33 - 67.33	1800	145022	0.571	0.137
		138600	6376465	4.166	1.000

CAUSATIVE FACTOR	FACTOR CLASS	LANDSLIDE PIXEL	CLASS PIXEL	FR	RF
ASPECT	Flat (-1)	4500	425727	0.485	0.050
	North (0 - 22.5)	10800	494388	1.002	0.104
	North-East (22.5 - 67.5)	8100	586242	0.634	0.066
	East (67.5 - 112.5)	17100	633343	1.239	0.128
	South-East (112.5 - 157.5)	22500	733766	1.407	0.145
	South (1575 - 202.5)	18900	783820	1.106	0.114
	South-West (202.5 - 247.5)	18900	843659	1.028	0.106

	West (247.5 - 292.5)	15300	716783	0.979	0.101
	North-West (292.5 - 337.5)	13500	599566	1.033	0.107
	North (337.5 - 360)	9000	541986	0.762	0.079
		138600	6359280	9.676	1.000

CAUSATIVE FACTOR	FACTOR CLASS	LANDSLIDE PIXEL	CLASS PIXEL	FR	RF
SPI	(-13.82) - (-9.05)	2700	873396	0.142	0.031
	(-9.05) - (-4.94)	37800	1197227	1.449	0.316
	(-4.94) - (-0.62)	27900	1606517	0.797	0.174
	(-0.62) - 2.19	57600	2035241	1.299	0.284
	2.19 - 13.76	12600	646899	0.894	0.195
		138600	6359280	4.580	1.000

CAUSATIVE FACTOR	FACTOR CLASS	LANDSLIDE PIXEL	CLASS PIXEL	FR	RF
TWI	(-8.28) - (-1.82)	40500	2028813	0.916	0.225
	(-1.82) - 2.40	60300	1722053	1.607	0.395
	2.40 - 5.22	28800	1643562	0.804	0.198
	5.22 - 9.22	8100	584932	0.635	0.156
	9.22 - 21.67	900	379920	0.109	0.027
		138600	6359280	4.071	1.000

CAUSATIVE FACTOR	FACTOR CLASS	LANDSLIDE PIXEL	CLASS PIXEL	FR	RF
DISTANCE TO RIVER (m)	0 - 8926.24	25200	1232644	0.947	0.197
	8926.24 - 17639.96	10800	1551405	0.322	0.067
	17639.97 - 26991.27	60300	1564846	1.784	0.371
	26991.28 - 37617.75	31500	1279540	1.140	0.237
	37617.76 - 54195.06	9900	747979	0.613	0.128
		137700	6376414	4.806	1.000

CAUSATIVE FACTOR	FACTOR CLASS	LANDSLIDE PIXEL	CLASS PIXEL	FR	RF
DISTANCE TO ROAD (m)	0 - 1210.12	108000	2790803	1.792	0.668
	1210.12 - 2860.28	21600	1844719	0.542	0.202
	2860.28 - 5005.5	8100	1071799	0.350	0.130
	5005.5 - 8415.84	0	510132	0.000	0.000
	8415.84 - 14026.4	0	158961	0.000	0.000
		137700	6376414	2.684	1.000

CAUSATIVE FACTOR	FACTOR CLASS	LANDSLIDE PIXEL	CLASS PIXEL	FR	RF
DISTANCE TO LINEAMENT (m)	0 - 1324.67	88200	2116170	1.930	0.556
	1324.68 - 2825.97	36000	1838453	0.907	0.261
	2825.97 - 4592.21	9900	1240895	0.369	0.106
	4592.22 - 6755.85	2700	805409	0.155	0.045
	6755.85 - 11259.76	900	375487	0.111	0.032
		137700	6376414	3.472	1.000

CAUSATIVE FACTOR	FACTOR CLASS	LANDSLIDE PIXEL	CLASS PIXEL	FR	RF
RAINFALL (mm)	669.53 - 743.01	0	421123	0.000	0.000
	743.02 - 816.48	0	461232	0.000	0.000
	816.49 - 889.96	9000	683791	0.609	0.171
	889.97 - 963.44	38700	956771	1.873	0.526
	963.45 - 1036.9	90000	3853499	1.082	0.303
		137700	6376416	3.564	1.000

CAUSATIVE FACTOR	FACTOR CLASS	LANDSLIDE PIXEL	CLASS PIXEL	FR	RF
LULC	WATER	0	252827	0.000	0.000
	TREES	77400	2987842	1.192	0.276
	FLOODED VEGETATION	0	615	0.000	0.000
	CROPS	3600	569119	0.291	0.067
	BUILT AREA	45900	896908	2.354	0.545
	BARE GROUND	0	216434	0.000	0.000
	SNOW/ ICE	0	332107	0.000	0.000
	CLOUDS	0	12	0.000	0.000
	RANGELAND	11700	1120288	0.480	0.111
		138600	6376152	4.317	1.000

CAUSATIVE FACTOR	FACTOR CLASS	LANDSLIDE PIXEL	CLASS PIXEL	FR	RF
GEOLOGY	QUATERNARY	2700	858197	0.145	0.009
	PLEISTOCENE	54900	2355382	1.072	0.069
	PROTEROZOIC	8100	220615	1.689	0.109
	PLIOCENE	33300	588364	2.604	0.169
	MIOCENE	12600	586602	0.988	0.064
	PALAEOZOIC	900	456370	0.091	0.006
	NEOPROTEROZOIC	1800	1006662	0.082	0.005
	MIOCENE	21600	124277	7.996	0.518
	PALAEOPROTEROZOIC	0	7913	0.000	0.000
	MIOCENE	2700	158597	0.783	0.051

	PALAEOZOIC	0	13492	0.000	0.000
		138600	6376471	15.451	1.000

CAUSATIVE FACTOR	FACTOR CLASS	LANDSLIDE PIXEL	CLASS PIXEL	FR	RF
LITHOLOGY	GRAVEL, PEBBLE, SAND, SILT AND CLAY	5400	248714	0.999	0.038
	DIAMICTITE, SHALE, SLATE, SANDSTONE, LIMESTONE	0	24227	0.000	0.000
	CARBONACEOUS SLATE, PHYLLITE, QUARTZITE	0	22410	0.000	0.000
	SILLIMANITE - KYANIE BEARING SCHIST, QUARTZITE	5400	137021	1.813	0.069
	SLATE,PHYLLITE,QUARTZARENITE, LIMESTONE,METABASICS	1800	991305	0.084	0.003
	GREY PHYLLITE, SCHIST AND QUARTZITE	900	41856	0.989	0.037
	LEUCOCRATIC GRANITE, APLITE, QUARTZ VEINS.	900	453565	0.091	0.003
	BIOTITE GRANITE	0	12666	0.000	0.000
	PINK, GREY DOLOMITE, PHYLLITE, SHALE.	0	1361	0.000	0.000
	SHALE, SLATE, QUARTZITE, CHERTY DOLOMITE	0	603	0.000	0.000
	DOLOMITE, SPORADIC QUARTZITE.	0	2675	0.000	0.000
	STREAKY AND BANDED GNEISS.	900	11094	3.732	0.141
	SALT GRIT, PURPLE GRIT,"LOKHAN"	0	1925	0.000	0.000
	THOLEIITIC BASALT MINOR QUARTZARENITE, SHALE	1800	17503	4.731	0.179
	MICACEOUS SANDSTONE, PURPLE CLAY, MUDSTONE	17100	635219	1.238	0.047
	GREY, PURPLE, RED SANDSTONE, SHALE, LIMESTONE	17100	164879	4.771	0.181
	BROWN SANDSTONE, RED CLAY, PURPLE CHOCOLATE SHALE	5400	85631	2.901	0.110
	GREY SAND, SILT AND CLAY	9900	384803	1.184	0.045
	COARSE SANDSTONE, BOULDER CONGLOMERATE, CLAY & GRIT	40500	1767380	1.054	0.040
	PINK, WHITE QUARTZITE, THIN BEDS OF RED SHALE.	0	435	0.000	0.000
	GREY MICACEOUS SANDSTONE, GRAVEL BEDS, SHALE, CLAY	28800	631037	2.100	0.079
	QUARTZITE, SHALE, SLATE, A FEW BASIC FLOWS.	0	4450	0.000	0.000
	SCHIST AND QUARTZITE	0	35	0.000	0.000

	CARBONACEOUS SLATE, PHYLLITE, LIMESTONE, QUARTZITE	0	394	0.000	0.000
	PINK, GREY LIMESTONE, SPORADIC SHALE.	0	383	0.000	0.000
	DOLOMITE, BRICK RED SHALE.	0	166	0.000	0.000
	OXIDISED SILT-CLAY WITH KANKAR AND MICACEOUS SAND	1800	565584	0.146	0.006
	GREY MICACEOUS SAND, SILT AND CLAY	0	98681	0.000	0.000
	ILL SORTED BOULDER, COBBLE,PEBBLE IN SANDY MATRIX	900	70214	0.590	0.022
	GREEN, CARBONACEOUS SHALE, LIMESTONE, QUARTZITE	0	255	0.000	0.000
		138600	6376471	26.424	1.000

The prediction rate for all the factors is calculated using Frequency Ratio is shown in Table. 5.2.

Table 5.2. Prediction rate for every factor using FR

CAUSATIVE FACTOR	PREDICTION RATE
ELEVATION	5.68
SLOPE	4.90
CURVATURE	4.05
ASPECT	1.00
SPI	2.99
TWI	3.86
RAINFALL	5.15
ROAD	7.00
RIVER	3.19
LINEAMENTS	5.49
LULC	5.72
GEOLOGY	5.43
LITHOLOGY	1.89

5.2. SHANNON'S ENTROPY

Shannon developed the information entropy, also known as the index entropy, to assess a system's disorder, unpredictability, and state of bewilderment [19], [15], [4]. This can be said to be the extended part of the FR. The importance of the factor is calculated for each causal factor and they are multiplied by the reclassified factors based on the reduced factor as calculated in the frequency ratio method. The mathematical expression for the above method can be expressed as:

$$E = -k \sum RF * Log (RF) \qquad (5.5)$$

$$W_i = \frac{1-E}{\sum(1-E)} \qquad (5.6)$$

Where, k = 1/ Log (m), E = Entropy, m = Number of classes in factor, W_i = Weights of every factor, i = activating factors

After doing the above calculations in the Excel sheet, LSM can be obtained in ArcGIS with the help of a raster calculator as show in equation 5.7.

$$LSM = \sum (Weights * FR_{maps}) \qquad (5.7)$$

The computational result for Shannon's Entropy for all the factors is shown in Table 5.3.

Table 5.3. Result of Shannon's Entropy for every activating factor

CAUSATIVE FACTOR	FACTOR CLASS	LANDSLIDE PIXEL	CLASS PIXEL	FR	RF	RF * log RF
ELEVATION (m)	196.25 - 728.15	72900	3356379	0.999	0.274	-0.1541
	728.15 - 1699.45	57600	1343257	1.973	0.542	-0.1443
	1699.46 - 2971.4	8100	555447	0.671	0.184	-0.1353
	2971.4 - 4035.2	0	514361	0.000	0.000	0
	4035.2 - 6093.44	0	607021	0.000	0.000	0
		138600	6376465	3.643	1.000	

CAUSATIVE FACTOR	FACTOR CLASS	LANDSLIDE PIXEL	CLASS PIXEL	FR	RF	RF * log RF
SLOPE (degree)	0 - 7.81	9900	2462173	0.184	0.032	-0.048
	7.81 - 17.43	40500	1634076	1.137	0.198	-0.139

	17.44 - 28.84	63000	1006603	2.872	0.500	-0.151
	28.85 - 41.46	22500	807769	1.278	0.222	-0.145
	41.47 - 76.61	2700	448659	0.276	0.048	-0.063
		138600	6359280	5.747	1.000	

CAUSATIVE FACTOR	FACTOR CLASS	LANDSLIDE PIXEL	CLASS PIXEL	FR	RF	RF * log RF
CURVATURE	(-40.44) - (-3.33)	0	150618	0.000	0.000	0.000
	(-3.33) - (-0.77)	23400	978213	1.101	0.264	-0.153
	(-0.77) - 0.66	79200	4126175	0.883	0.212	-0.143
	0.66 - 3.33	34200	976437	1.611	0.387	-0.160
	3.33 - 67.33	1800	145022	0.571	0.137	-0.118
		138600	6376465	4.166	1.000	

CAUSATIVE FACTOR	FACTOR CLASS	LANDSLIDE PIXEL	CLASS PIXEL	FR	RF	RF * log RF
ASPECT	Flat (-1)	4500	425727	0.485	0.050	-0.065
	North (0 - 22.5)	10800	494388	1.002	0.104	-0.102
	North-East (22.5 - 67.5)	8100	586242	0.634	0.066	-0.078
	East (67.5 - 112.5)	17100	633343	1.239	0.128	-0.114
	South-East (112.5 - 157.5)	22500	733766	1.407	0.145	-0.122
	South (1575 - 202.5)	18900	783820	1.106	0.114	-0.108
	South-West (202.5 - 247.5)	18900	843659	1.028	0.106	-0.103
	West (247.5 - 292.5)	15300	716783	0.979	0.101	-0.101
	North-West (292.5 - 337.5)	13500	599566	1.033	0.107	-0.104
	North (337.5 - 360)	9000	541986	0.762	0.079	-0.087
		138600	6359280	9.676	1.000	

CAUSATIVE FACTOR	FACTOR CLASS	LANDSLIDE PIXEL	CLASS PIXEL	FR	RF	RF * log RF
SPI	(-13.82) - (-9.05)	2700	873396	0.142	0.031	-0.047
	(-9.05) - (-4.94)	37800	1197227	1.449	0.316	-0.158
	(-4.94) - (-0.62)	27900	1606517	0.797	0.174	-0.132
	(-0.62) - 2.19	57600	2035241	1.299	0.284	-0.155
	2.19 - 13.76	12600	646899	0.894	0.195	-0.138
		138600	6359280	4.580	1.000	

CAUSATIVE FACTOR	FACTOR CLASS	LANDSLIDE PIXEL	CLASS PIXEL	FR	RF	RF * log RF
TWI	(-8.28) - (-1.82)	40500	2028813	0.916	0.225	-0.146
	(-1.82) - 2.40	60300	1722053	1.607	0.395	-0.159
	2.40 - 5.22	28800	1643562	0.804	0.198	-0.139
	5.22 - 9.22	8100	584932	0.635	0.156	-0.126
	9.22 - 21.67	900	379920	0.109	0.027	-0.042
		138600	6359280	4.071	1.000	

CAUSATIVE FACTOR	FACTOR CLASS	LANDSLIDE PIXEL	CLASS PIXEL	FR	RF	RF * log RF
DISTANCE TO RIVER (m)	0 - 8926.24	25200	1232644	0.947	0.197	-0.139
	8926.24 - 17639.96	10800	1551405	0.322	0.067	-0.079
	17639.97 - 26991.27	60300	1564846	1.784	0.371	-0.160
	26991.28 - 37617.75	31500	1279540	1.140	0.237	-0.148
	37617.76 - 54195.06	9900	747979	0.613	0.128	-0.114
		137700	6376414	4.806	1.000	

CAUSATIVE FACTOR	FACTOR CLASS	LANDSLIDE PIXEL	CLASS PIXEL	FR	RF	RF * log RF
DISTANCE TO ROAD (m)	0 - 1210.12	108000	2790803	1.792	0.668	-0.117
	1210.12 - 2860.28	21600	1844719	0.542	0.202	-0.140
	2860.28 - 5005.5	8100	1071799	0.350	0.130	-0.115
	5005.5 - 8415.84	0	510132	0.000	0.000	0.000
	8415.84 - 14026.4	0	158961	0.000	0.000	0.000
		137700	6376414	2.684	1.000	

CAUSATIVE FACTOR	FACTOR CLASS	LANDSLIDE PIXEL	CLASS PIXEL	FR	RF	RF * log RF
DISTANCE TO LINEAMENT (m)	0 - 1324.67	88200	2116170	1.930	0.556	-0.142
	1324.68 - 2825.97	36000	1838453	0.907	0.261	-0.152
	2825.97 - 4592.21	9900	1240895	0.369	0.106	-0.104
	4592.22 - 6755.85	2700	805409	0.155	0.045	-0.060
	6755.85 - 11259.76	900	375487	0.111	0.032	-0.048
		137700	6376414	3.472	1.000	

CAUSATIVE FACTOR	FACTOR CLASS	LANDSLIDE PIXEL	CLASS PIXEL	FR	RF	RF * log RF
RAINFALL (mm)	669.53 - 743.01	0	421123	0.000	0.000	0.000
	743.02 - 816.48	0	461232	0.000	0.000	0.000
	816.49 - 889.96	9000	683791	0.609	0.171	-0.131
	889.97 - 963.44	38700	956771	1.873	0.526	-0.147
	963.45 - 1036.9	90000	3853499	1.082	0.303	-0.157
		137700	6376416	3.564	1.000	

CAUSATIVE FACTOR	FACTOR CLASS	LANDSLIDE PIXEL	CLASS PIXEL	FR	RF	RF * log RF
LULC	WATER	0	252827	0.000	0.000	0.000
	TREES	77400	2987842	1.192	0.276	-0.154
	FLOODED VEGETATION	0	615	0.000	0.000	0.000
	CROPS	3600	569119	0.291	0.067	-0.079
	BUILT AREA	45900	896908	2.354	0.545	-0.144
	BARE GROUND	0	216434	0.000	0.000	0.000
	SNOW/ ICE	0	332107	0.000	0.000	0.000
	CLOUDS	0	12	0.000	0.000	0.000
	RANGELAND	11700	1120288	0.480	0.111	-0.106
		138600	6376152	4.317	1.000	

CAUSATIVE FACTOR	FACTOR CLASS	LANDSLIDE PIXEL	CLASS PIXEL	FR	RF	RF * log RF
GEOLOGY	QUATERNARY	2700	858197	0.145	0.009	-0.019
	PLEISTOCENE	54900	2355382	1.072	0.069	-0.080
	PROTEROZOIC	8100	220615	1.689	0.109	-0.105
	PLIOCENE	33300	588364	2.604	0.169	-0.130
	MIOCENE	12600	586602	0.988	0.064	-0.076
	PALAEOZOIC	900	456370	0.091	0.006	-0.013
	NEOPROTEROZOIC	1800	1006662	0.082	0.005	-0.012
	MIOCENE	21600	124277	7.996	0.518	-0.148
	PALAEOPROTEROZOIC	0	7913	0.000	0.000	0.000
	MIOCENE	2700	158597	0.783	0.051	-0.066
	PALAEOZOIC	0	13492	0.000	0.000	0.000
		138600	6376471	15.451	1.000	

CAUSATIVE FACTOR	FACTOR CLASS	LANDSLIDE PIXEL	CLASS PIXEL	FR	RF	RF * log RF
LITHOLOGY	GRAVEL, PEBBLE, SAND, SILT AND CLAY	5400	248714	0.999	0.038	-0.153
	DIAMICTITE, SHALE, SLATE, SANDSTONE, LIMESTONE	0	24227	0.000	0.000	0.000
	CARBONACEOUS SLATE, PHYLLITE, QUARTZITE	0	22410	0.000	0.000	0.000
	SILLIMANITE - KYANIE BEARING SCHIST, QUARTZITE	5400	137021	1.813	0.069	-0.152
	SLATE, PHYLLITE,QUARTZARENITE, LIMESTONE,METABASICS	1800	991305	0.084	0.003	-0.037
	GREY PHYLLITE, SCHIST AND QUARTZITE	900	41856	0.989	0.037	-0.153
	LEUCOCRATIC GRANITE, APLITE, QUARTZ VEINS.	900	453565	0.091	0.003	-0.039
	BIOTITE GRANITE	0	12666	0.000	0.000	0.000
	PINK, GREY DOLOMITE, PHYLLITE, SHALE.	0	1361	0.000	0.000	0.000
	SHALE, SLATE, QUARTZITE, CHERTY DOLOMITE	0	603	0.000	0.000	0.000
	DOLOMITE, SPORADIC QUARTZITE.	0	2675	0.000	0.000	0.000
	STREAKY AND BANDED GNEISS.	900	11094	3.732	0.141	0.000
	SALT GRIT, PURPLE GRIT,"LOKHAN"	0	1925	0.000	0.000	0.000
	THOLEIITIC BASALT MINOR QUARTZARENITE, SHALE	1800	17503	4.731	0.179	0.131
	MICACEOUS SANDSTONE, PURPLE CLAY, MUDSTONE	17100	635219	1.238	0.047	-0.159
	GREY, PURPLE, RED SANDSTONE, SHALE, LIMESTONE	17100	164879	4.771	0.181	0.136
	BROWN SANDSTONE, RED CLAY, PURPLE CHOCOLATE SHALE	5400	85631	2.901	0.110	-0.085
	GREY SAND, SILT AND CLAY	9900	384803	1.184	0.045	-0.158
	COARSE SANDSTONE, BOULDER CONGLOMERATE,CLAY & GRIT	40500	1767380	1.054	0.040	-0.155
	PINK, WHITE QUARTZITE, THIN BEDS OF RED SHALE.	0	435	0.000	0.000	0.000
	GREY MICACEOUS SANDSTONE, GRAVEL BEDS, SHALE, CLAY	28800	631037	2.100	0.079	-0.141

	QUARTZITE, SHALE, SLATE, A FEW BASIC FLOWS.	0	4450	0.000	0.000	0.000
	SCHIST AND QUARTZITE	0	35	0.000	0.000	0.000
	CARBONACEOUS SLATE, PHYLLITE, LIMESTONE, QUARTZITE	0	394	0.000	0.000	0.000
	PINK, GREY LIMESTONE, SPORADIC SHALE.	0	383	0.000	0.000	0.000
	DOLOMITE, BRICK RED SHALE.	0	166	0.000	0.000	0.000
	OXIDISED SILT-CLAY WITH KANKAR AND MICACEOUS SAND	1800	565584	0.146	0.006	-0.055
	GREY MICACEOUS SAND, SILT AND CLAY	0	98681	0.000	0.000	0.000
	ILL SORTED BOULDER,COBBLE,PEBBLE IN SANDY MATRIX	900	70214	0.590	0.022	-0.127
	GREEN, CARBONACEOUS SHALE, LIMESTONE, QUARTZITE	0	255	0.000	0.000	0.000
		138600	6376471	26.424	1.000	

The calculation and weights for Shannon's Entropy is shown in Table 5.4.

Table 5.4. Weights for every factor using Shannon's Entropy

CAUSATIVE FACTOR	m	k	Ej	1 - Ej	Wi
ELEVATION	5	1.431	0.620	0.380	0.1145
SLOPE	5	1.431	0.782	0.218	0.0659
CURVATURE	5	1.431	0.820	0.180	0.0542
ASPECT	10	1.000	0.983	0.017	0.0051
SPI	5	1.431	0.902	0.098	0.0295
TWI	5	1.431	0.876	0.124	0.0375
RIVER	5	1.431	0.915	0.085	0.0256
ROAD	5	1.431	0.533	0.467	0.1408
LINEAMENTS	5	1.431	0.724	0.276	0.0834
RAINFALL	5	1.431	0.623	0.377	0.1139
LULC	9	1.048	0.506	0.494	0.1490
GEOLOGY	11	0.960	0.624	0.376	0.1134
LITHOLOGY	30	0.677	0.777	0.223	0.0674
				3.314	

5.3. INFORMATION VALUE

The IV model is a bivariate statistical strategy for predicting the geographical relationship between landslides and their component classes [38], [40], [3]. The approach is first put out by Yin and Yan. The value of IV above 0 represents a greater likelihood of an event whereas the value of IV below 0 represents a lower likelihood of the event of a landslide [31]. The calculation is done using equation 5.8.

$$I = \ln [(N_L/N_C)/(N_{TL}/N_{CL})] \qquad (5.8)$$

where,

N_{CL} = the map's overall pixel

N_{TL} = total pixel with landslides

N_C = class pixel

N_L = landslides pixels in class

After doing the above calculations in the Excel sheet, LSM can be obtained in ArcGIS by using Raster Calculator as follows:

$$LSM = \sum (IV_{maps}) \qquad (5.9)$$

The computational result for Information Value for all the factors is shown in Table 5.5.

Table 5.5. Result of Information Value for every activating factor

CAUSATIVE FACTOR	FACTOR CLASS	LANDSLIDE PIXEL	CLASS PIXEL	IV
ELEVATION (m)	196.25 - 728.15	72900	3356379	-0.001
	728.15 - 1699.45	57600	1343257	0.679
	1699.46 - 2971.4	8100	555447	-0.399
	2971.4 - 4035.2	0	514361	0.000
	4035.2 - 6093.44	0	607021	0.000
		138600	6376465	

CAUSATIVE FACTOR	FACTOR CLASS	LANDSLIDE PIXEL	CLASS PIXEL	IV
SLOPE (degree)	0 - 7.81	9900	2462173	-1.690
	7.81 - 17.43	40500	1634076	0.129

	17.44 - 28.84	63000	1006603	1.055
	28.85 - 41.46	22500	807769	0.245
	41.47 - 76.61	2700	448659	-1.287
		138600	6359280	

CAUSATIVE FACTOR	FACTOR CLASS	LANDSLIDE PIXEL	CLASS PIXEL	IV
CURVATURE	(-40.44) - (-3.33)	0	150618	0.000
	(-3.33) - (-0.77)	23400	978213	0.096
	(-0.77) - 0.66	79200	4126175	-0.124
	0.66 - 3.33	34200	976437	0.477
	3.33 - 67.33	1800	145022	-0.560
		138600	6376465	

CAUSATIVE FACTOR	FACTOR CLASS	LANDSLIDE PIXEL	CLASS PIXEL	IV
ASPECT	Flat (-1)	4500	425727	-0.724
	North (0 - 22.5)	10800	494388	0.002
	North-East (22.5 - 67.5)	8100	586242	-0.456
	East (67.5 - 112.5)	17100	633343	0.214
	South-East (112.5 - 157.5)	22500	733766	0.341
	South (1575 - 202.5)	18900	783820	0.101
	South-West (202.5 - 247.5)	18900	843659	0.027
	West (247.5 - 292.5)	15300	716783	-0.021
	North-West (292.5 - 337.5)	13500	599566	0.033
	North (337.5 - 360)	9000	541986	-0.272
		138600	6359280	

CAUSATIVE FACTOR	FACTOR CLASS	LANDSLIDE PIXEL	CLASS PIXEL	IV
SPI	(-13.82) - (-9.05)	2700	873396	-1.953
	(-9.05) - (-4.94)	37800	1197227	0.371
	(-4.94) - (-0.62)	27900	1606517	-0.227
	(-0.62) - 2.19	57600	2035241	0.261
	2.19 - 13.76	12600	646899	-0.112
		138600	6359280	

CAUSATIVE FACTOR	FACTOR CLASS	LANDSLIDE PIXEL	CLASS PIXEL	IV
TWI	(-8.28) - (-1.82)	40500	2028813	-0.088
	(-1.82) - 2.40	60300	1722053	0.474
	2.40 - 5.22	28800	1643562	-0.218
	5.22 - 9.22	8100	584932	-0.454
	9.22 - 21.67	900	379920	-2.219
		138600	6359280	

CAUSATIVE FACTOR	FACTOR CLASS	LANDSLIDE PIXEL	CLASS PIXEL	IV
DISTANCE TO RIVER (m)	0 - 8926.24	25200	1232644	-0.055
	8926.24 - 17639.96	10800	1551405	-1.132
	17639.97 - 26991.27	60300	1564846	0.579
	26991.28 - 37617.75	31500	1279540	0.131
	37617.76 - 54195.06	9900	747979	-0.490
		137700	6376414	

CAUSATIVE FACTOR	FACTOR CLASS	LANDSLIDE PIXEL	CLASS PIXEL	IV
DISTANCE TO ROAD (m)	0 - 1210.12	108000	2790803	0.583
	1210.12 - 2860.28	21600	1844719	-0.612
	2860.28 - 5005.5	8100	1071799	-1.050
	5005.5 - 8415.84	0	510132	0.000
	8415.84 - 14026.4	0	158961	0.000
		137700	6376414	

CAUSATIVE FACTOR	FACTOR CLASS	LANDSLIDE PIXEL	CLASS PIXEL	IV
DISTANCE TO LINEAMENT (m)	0 - 1324.67	88200	2116170	0.658
	1324.68 - 2825.97	36000	1838453	-0.098
	2825.97 - 4592.21	9900	1240895	-0.996
	4592.22 - 6755.85	2700	805409	-1.863
	6755.85 - 11259.76	900	375487	-2.198
		137700	6376414	

CAUSATIVE FACTOR	FACTOR CLASS	LANDSLIDE PIXEL	CLASS PIXEL	IV
RAINFALL (mm)	669.53 - 743.01	0	421123	0.000
	743.02 - 816.48	0	461232	0.000
	816.49 - 889.96	9000	683791	-0.495
	889.97 - 963.44	38700	956771	0.628

	963.45 - 1036.9	90000	3853499	0.078
		137700	6376416	

CAUSATIVE FACTOR	FACTOR CLASS	LANDSLIDE PIXEL	CLASS PIXEL	IV
LULC	WATER	0	252827	0.000
	TREES	77400	2987842	0.175
	FLOODED VEGETATION	0	615	0.000
	CROPS	3600	569119	-1.234
	BUILT AREA	45900	896908	0.856
	BARE GROUND	0	216434	0.000
	SNOW/ ICE	0	332107	0.000
	CLOUDS	0	12	0.000
	RANGELAND	11700	1120288	-0.733
		138600	6376152	

CAUSATIVE FACTOR	FACTOR CLASS	LANDSLIDE PIXEL	CLASS PIXEL	IV
GEOLOGY	QUATERNARY	2700	858197	-1.933
	PLEISTOCENE	54900	2355382	0.070
	PROTEROZOIC	8100	220615	0.524
	PLIOCENE	33300	588364	0.957
	MIOCENE	12600	586602	-0.012
	PALAEOZOIC	900	456370	-2.400
	NEOPROTEROZOIC	1800	1006662	-2.498
	MIOCENE	21600	124277	2.079
	PALAEOPROTEROZOIC	0	7913	0.000
	MIOCENE	2700	158597	-0.244
	PALAEOZOIC	0	13492	0.000
		138600	6376471	

CAUSATIVE FACTOR	FACTOR CLASS	LANDSLIDE PIXEL	CLASS PIXEL	IV
LITHOLOGY	GRAVEL, PEBBLE, SAND, SILT AND CLAY	5400	248714	-0.001
	DIAMICTITE, SHALE, SLATE, SANDSTONE, LIMESTONE	0	24227	0.000
	CARBONACEOUS SLATE, PHYLLITE, QUARTZITE	0	22410	0.000
	SILLIMANITE - KYANIE BEARING SCHIST, QUARTZITE	5400	137021	0.595
	SLATE,PHYLLITE,QUARTZARENITE, LIMESTONE,METABASICS	1800	991305	-2.482

	GREY PHYLLITE, SCHIST AND QUARTZITE	900	41856	-0.011
	LEUCOCRATIC GRANITE, APLITE, QUARTZ VEINS.	900	453565	-2.394
	BIOTITE GRANITE	0	12666	0.000
	PINK, GREY DOLOMITE, PHYLLITE, SHALE.	0	1361	0.000
	SHALE, SLATE, QUARTZITE, CHERTY DOLOMITE	0	603	0.000
	DOLOMITE, SPORADIC QUARTZITE.	0	2675	0.000
	STREAKY AND BANDED GNEISS.	900	11094	1.317
	SALT GRIT, PURPLE GRIT,"LOKHAN"	0	1925	0.000
	THOLEIITIC BASALT MINOR QUARTZARENITE, SHALE	1800	17503	1.554
	MICACEOUS SANDSTONE, PURPLE CLAY, MUDSTONE	17100	635219	0.214
	GREY, PURPLE, RED SANDSTONE, SHALE, LIMESTONE	17100	164879	1.563
	BROWN SANDSTONE, RED CLAY, PURPLE CHOCOLATE SHALE	5400	85631	1.065
	GREY SAND, SILT AND CLAY	9900	384803	0.169
	COARSE SANDSTONE, BOULDER CONGLOMERATE,CLAY & GRIT	40500	1767380	0.053
	PINK, WHITE QUARTZITE, THIN BEDS OF RED SHALE.	0	435	0.000
	GREY MICACEOUS SANDSTONE, GRAVEL BEDS, SHALE, CLAY	28800	631037	0.742
	QUARTZITE, SHALE, SLATE, A FEW BASIC FLOWS.	0	4450	0.000
	SCHIST AND QUARTZITE	0	35	0.000
	CARBONACEOUS SLATE, PHYLLITE, LIMESTONE, QUARTZITE	0	394	0.000
	PINK, GREY LIMESTONE, SPORADIC SHALE.	0	383	0.000
	DOLOMITE, BRICK RED SHALE.	0	166	0.000
	OXIDISED SILT-CLAY WITH KANKAR AND MICACEOUS SAND	1800	565584	-1.921
	GREY MICACEOUS SAND, SILT AND CLAY	0	98681	0.000
	ILL SORTED BOULDER,COBBLE,PEBBLE IN SANDY MATRIX	900	70214	-0.528
	GREEN, CARBONACEOUS SHALE, LIMESTONE, QUARTZITE	0	255	0.000
		138600	6376471	

5.4. WEIGHT OF EVIDENCE

The WoE approach is a statistical methodology used in the mapping of landslide vulnerability [11]. The technique is based on the notion of comparing the likelihood of a landslide in a certain location against the likelihood of its absence [17]. The approach analyses the likelihood ratio of landslide likelihood to non-likelihood in a particular place and then assigns a weight to each component that activates to the probability ratio [13], [1], [30], [5].

For calculation purposes, some values need to be calculated. The values are:

$$N_1 = N_L$$

$$N_2 = N_{TL} - N_L$$

$$N_3 = N_C - N_L$$

$$N_4 = N_{CL} - N_{TL} - N_C + N_L$$

$$W^+ = \ln \frac{\frac{N_1}{N_1 + N_2}}{\frac{N_3}{N_3 + N_4}} \qquad (5.10)$$

$$W^- = \ln \frac{\frac{N_2}{N_1 + N_2}}{\frac{N_4}{N_3 + N_4}} \qquad (5.11)$$

where,

N_1 = pixels of landslide on a factor class,

N_2 = pixels of landslide absent from a factor class,

N_3 = pixels in a particular factor class that do not include any pixels from landslides and class

N_4 = pixels where the provided factor and the landslide are absent

N_{CL} = the map's overall pixel

N_{TL} = total pixel with landslides

N_C = class pixel

N_L = landslides pixels in class

These values are used to arrive at the extent of C for the given vulnerability variable.

$$C = W^+ - W^- \qquad (5.12)$$

where,

C = contrast value

W^+ = weight allocated to a certain raster indicating the impact of a factor class

W^- = weight allocated under the absence of factor class

The negative value of C represents the lesser chances of landslide occurrence whereas the positive value represents a high occurrence probability [37], [39].

After doing the above calculations in the Excel sheet, LSM can be obtained in ArcGIS with the help of Raster Calculator as follows:

$$LSM = \sum (C_{maps}) \qquad (5.13)$$

The computational result for Weight of Evidence for all the factors is shown in Table 5.6.

Table 5.6. Result of Weight of Evidence for every activating factor

CAUSATIVE FACTOR	FACTOR CLASS	LANDSLIDE PIXEL	CLASS PIXEL	W+	W-	C
ELEVATION (m)	196.25 - 728.15	72900	3356379	-0.001	0.001	-0.002
	728.15 - 1699.45	57600	1343257	0.701	-0.306	1.008
	1699.46 - 2971.4	8100	555447	-0.406	0.032	-0.438
	2971.4 - 4035.2	0	514361	0.000	0.086	0.000
	4035.2 - 6093.44	0	607021	0.000	0.102	0.000
		138600	6376465			

CAUSATIVE FACTOR	FACTOR CLASS	LANDSLIDE PIXEL	CLASS PIXEL	W+	W-	C
SLOPE (degree)	0 - 7.81	9900	2462173	-1.708	0.427	-2.135
	7.81 - 17.43	40500	1634076	0.132	-0.050	0.181
	17.44 - 28.84	63000	1006603	1.097	-0.442	1.539
	28.85 - 41.46	22500	807769	0.252	-0.042	0.294
	41.47 - 76.61	2700	448659	-1.303	0.055	-1.358
		138600	6359280			

CAUSATIVE FACTOR	FACTOR CLASS	LANDSLIDE PIXEL	CLASS PIXEL	W+	W-	C
CURVATURE	(-40.44) - (-3.33)	0	150618	0.000	0.024	0.000
	(-3.33) - (-0.77)	23400	978213	0.098	-0.019	0.117
	(-0.77) - 0.66	79200	4126175	-0.127	0.199	-0.326
	0.66 - 3.33	34200	976437	0.491	-0.120	0.610
	3.33 - 67.33	1800	145022	-0.570	0.010	-0.580
		138600	6376465			

CAUSATIVE FACTOR	FACTOR CLASS	LANDSLIDE PIXEL	CLASS PIXEL	W+	W-	C
ASPECT	Flat (-1)	4500	425727	-0.736	0.037	-0.774
	North (0 - 22.5)	10800	494388	-0.001	0.000	-0.001
	North-East (22.5 - 67.5)	8100	586242	-0.467	0.038	-0.504
	East (67.5 - 112.5)	17100	633343	0.214	-0.027	0.241
	South-East (112.5 - 157.5)	22500	733766	0.343	-0.055	0.398
	South (1575 - 202.5)	18900	783820	0.097	-0.015	0.112
	South-West (202.5 - 247.5)	18900	843659	0.022	-0.003	0.025
	West (247.5 - 292.5)	15300	716783	-0.026	0.003	-0.030
	North-West (292.5 - 337.5)	13500	599566	0.029	-0.003	0.032
	North (337.5 - 360)	9000	541986	-0.280	0.023	-0.303
		138600	6359280			

CAUSATIVE FACTOR	FACTOR CLASS	LANDSLIDE PIXEL	CLASS PIXEL	W+	W-	C
SPI	(-13.82) - (-9.05)	2700	873396	-1.972	0.131	-2.103
	(-9.05) - (-4.94)	37800	1197227	0.381	-0.112	0.493
	(-4.94) - (-0.62)	27900	1606517	0.000	0.068	-0.068
	(-0.62) - 2.19	57600	2035241	0.000	-0.155	0.155
	2.19 - 13.76	12600	646899	0.000	0.012	-0.012
		138600	6359280			

CAUSATIVE FACTOR	FACTOR CLASS	LANDSLIDE PIXEL	CLASS PIXEL	W+	W-	C
TWI	(-8.28) - (-1.82)	40500	2028813	-0.090	0.040	-0.129
	(-1.82) - 2.40	60300	1722053	0.488	-0.260	0.748
	2.40 - 5.22	28800	1643562	-0.223	0.068	-0.290
	5.22 - 9.22	8100	584932	-0.462	0.037	-0.499
	9.22 - 21.67	900	379920	-2.239	0.056	-2.295
		138600	6359280			

CAUSATIVE FACTOR	FACTOR CLASS	LANDSLIDE PIXEL	CLASS PIXEL	W+	W-	C
DISTANCE TO RIVER (m)	0 - 8926.24	25200	1232644	-0.056	0.013	-0.069
	8926.24 - 17639.96	10800	1551405	-1.147	0.202	-1.349
	17639.97 - 26991.27	60300	1564846	0.597	-0.300	0.897
	26991.28 - 37617.75	31500	1279540	0.134	-0.037	0.171
	37617.76 - 54195.06	9900	747979	-0.498	0.051	-0.549
		137700	6376414			

CAUSATIVE FACTOR	FACTOR CLASS	LANDSLIDE PIXEL	CLASS PIXEL	W+	W-	C
DISTANCE TO ROAD (m)	0 - 1210.12	108000	2790803	0.601	-0.972	1.573
	1210.12 - 2860.28	21600	1844719	-0.622	0.175	-0.797
	2860.28 - 5005.5	8100	1071799	-1.064	0.126	-1.190
	5005.5 - 8415.84	0	510132	0.000	0.085	0.000
	8415.84 - 14026.4	0	158961	0.000	0.026	0.000
		137700	6376414			

CAUSATIVE FACTOR	FACTOR CLASS	LANDSLIDE PIXEL	CLASS PIXEL	W+	W-	C
DISTANCE TO LINEAMENT (m)	0 - 1324.67	88200	2116170	0.678	-0.630	1.308
	1324.68 - 2825.97	36000	1838453	-0.100	0.038	-0.138
	2825.97 - 4592.21	9900	1240895	-1.010	0.145	-1.155
	4592.22 - 6755.85	2700	805409	-1.881	0.118	-1.999
	6755.85 - 11259.76	900	375487	-2.218	0.055	-2.273
		137700	6376414			

CAUSATIVE FACTOR	FACTOR CLASS	LANDSLIDE PIXEL	CLASS PIXEL	W+	W-	C
RAINFALL (mm)	669.53 - 743.01	0	421123	0.000	0.070	0.000
	743.02 - 816.48	0	461232	0.000	0.077	0.000
	816.49 - 889.96	9000	683791	-0.504	0.047	-0.551
	889.97 - 963.44	38700	956771	0.647	-0.171	0.818
	963.45 - 1036.9	90000	3853499	0.080	-0.136	0.216
		137700	6376416			

CAUSATIVE FACTOR	FACTOR CLASS	LANDSLIDE PIXEL	CLASS PIXEL	W+	W-	C
LULC	WATER	0	252827	0.000	0.041	0.000
	TREES	77400	2987842	0.180	-0.189	0.369
	FLOODED VEGETATION	0	615	0.000	0.000	0.000
	CROPS	3600	569119	-1.250	0.069	-1.319
	BUILT AREA	45900	896908	0.887	-0.256	1.142
	BARE GROUND	0	216434	0.000	0.035	0.000
	SNOW/ ICE	0	332107	0.000	0.055	0.000
	CLOUDS	0	12	0.000	0.000	0.000
	RANGELAND	11700	1120288	-0.745	0.107	-0.852
		138600	6376152			

CAUSATIVE FACTOR	FACTOR CLASS	LANDSLIDE PIXEL	CLASS PIXEL	W+	W-	C
GEOLOGY	QUATERNARY	2700	858197	-1.952	0.128	-2.079
	PLEISTOCENE	54900	2355382	0.071	-0.044	0.116
	PROTEROZOIC	8100	220615	0.540	-0.026	0.565
	PLIOCENE	33300	588364	0.993	-0.182	1.175
	MIOCENE	12600	586602	-0.012	0.001	-0.013
	PALAEOZOIC	900	456370	-2.420	0.069	-2.489
	NEOPROTEROZOIC	1800	1006662	-2.518	0.163	-2.681
	MIOCENE	21600	124277	2.248	-0.153	2.401
	PALAEOPROTEROZOIC	0	7913	0.000	0.001	0.000
	MIOCENE	2700	158597	-0.249	0.006	-0.255
	PALAEOZOIC	0	13492	0.000	0.002	0.000
		138600	6376471			

CAUSATIVE FACTOR	FACTOR CLASS	LAND SLIDE PIXEL	CLASS PIXEL	W+	W-	C
LITHOLOGY	GRAVEL, PEBBLE, SAND, SILT AND CLAY	5400	248714	-0.001	0.000	-0.001
	DIAMICTITE, SHALE, SLATE, SANDSTONE, LIMESTONE	0	24227	0.000	0.004	0.000
	CARBONACEOUS SLATE, PHYLLITE, QUARTZITE	0	22410	0.000	0.004	0.000
	SILLIMANITE - KYANIE BEARING SCHIST, QUARTZITE	5400	137021	0.613	-0.018	0.632
	SLATE,PHYLLITE,QUARTZ ARENITE, LIMESTONE,METABASICS	1800	991305	-2.503	0.160	-2.662
	GREY PHYLLITE, SCHIST AND QUARTZITE	900	41856	-0.011	0.000	-0.011
	LEUCOCRATIC GRANITE, APLITE, QUARTZ VEINS.	900	453565	-2.414	0.069	-2.483

	BIOTITE GRANITE	0	12666	0.000	0.002	0.000
	PINK, GREY DOLOMITE, PHYLLITE, SHALE.	0	1361	0.000	0.000	0.000
	SHALE, SLATE, QUARTZITE, CHERTY DOLOMITE	0	603	0.000	0.000	0.000
	DOLOMITE, SPORADIC QUARTZITE.	0	2675	0.000	0.000	0.000
	STREAKY AND BANDED GNEISS.	900	11094	1.380	-0.005	1.385
	SALT GRIT, PURPLE GRIT,"LOKHAN"	0	1925	0.000	0.000	0.000
	THOLEIITIC BASALT MINOR QUARTZARENITE, SHALE	1800	17503	1.641	-0.011	1.651
	MICACEOUS SANDSTONE, PURPLE CLAY, MUDSTONE	17100	635219	0.219	-0.027	0.247
	GREY, PURPLE, RED SANDSTONE, SHALE, LIMESTONE	17100	164879	1.650	-0.108	1.758
	BROWN SANDSTONE, RED CLAY, PURPLE CHOCOLATE SHALE	5400	85631	1.108	-0.027	1.135
	GREY SAND, SILT AND CLAY	9900	384803	0.173	-0.012	0.185
	COARSE SANDSTONE, BOULDER CONGLOMERATE,CLAY & GRIT	40500	1767380	0.054	-0.021	0.076
	PINK, WHITE QUARTZITE, THIN BEDS OF RED SHALE.	0	435	0.000	0.000	0.000
	GREY MICACEOUS SANDSTONE, GRAVEL BEDS, SHALE, CLAY	28800	631037	0.767	-0.131	0.898
	QUARTZITE, SHALE, SLATE, A FEW BASIC FLOWS.	0	4450	0.000	0.001	0.000
	SCHIST AND QUARTZITE	0	35	0.000	0.000	0.000
	CARBONACEOUS SLATE, PHYLLITE, LIMESTONE, QUARTZITE	0	394	0.000	0.000	0.000
	PINK, GREY LIMESTONE, SPORADIC SHALE.	0	383	0.000	0.000	0.000
	DOLOMITE, BRICK RED SHALE.	0	166	0.000	0.000	0.000
	OXIDISED SILT-CLAY WITH KANKAR AND MICACEOUS SAND	1800	565584	-1.940	0.082	-2.022
	GREY MICACEOUS SAND, SILT AND CLAY	0	98681	0.000	0.016	0.000
	ILL SORTED BOULDER,COBBLE,PEBBLE IN SANDY MATRIX	900	70214	-0.537	0.005	-0.542
	GREEN, CARBONACEOUS SHALE, LIMESTONE, QUARTZITE	0	255	0.000	0.000	0.000
		138600	6376471			

5.5. CERTAINTY FACTOR

The certainty factor technique is a favorability function for addressing the difficulty of merging heterogeneous data [36]. Depending on the method's use, data or expert judgment may be used. Our study is driven by data. The CF is described for each data layer as the difference between the prior likelihood of a landslide occurring in the research area and the subsequent certainty that the claim is true.

$$CF_{ij} = \frac{aij - a}{aij\,(1-a)} \text{ if } a_{ij} \geq a \qquad (5.14)$$

$$CF_{ij} = \frac{aij - a}{a\,(1-aij)} \text{ if } a_{ij} \leq a \qquad (5.15)$$

where,

a_{ij} = conditional probability; a = prior probability

$$\text{Conditional probability} = \frac{\text{landslide pixel of certain class}}{\text{class pixel of certain class}} \qquad (5.16)$$

$$\text{Prior probability} = \frac{\text{total landslide pixel}}{\text{total class pixel}} \qquad (5.17)$$

The range of certainty factor lies between -1 to 1 where a negative value points to lower certitude in the event of a landslide and a positive value points to higher certitude in the event of a landslide.

After doing the above calculations in the Excel sheet, LSM can be obtained in ArcGIS with the help of Raster Calculator as follows:

$$LSM = \sum (CF_{maps}) \qquad (5.18)$$

The computational result for Certainty Factor for all the factors is shown in Table 5.7.

Table 5.7. Result of Certainty Factor for every activating factor

CAUSATIVE FACTOR	FACTOR CLASS	LANDSLIDE PIXEL	CLASS PIXEL	CP	PP	CF
ELEVATION (m)	196.25 - 728.15	72900	3356379	0.0217	0.0217	-0.0008
	728.15 - 1699.45	57600	1343257	0.0429	0.0217	0.5041
	1699.46 - 2971.4	8100	555447	0.0146	0.0217	-0.3340
	2971.4 - 4035.2	0	514361	0.0000	0.0217	-1.0000
	4035.2 - 6093.44	0	607021	0.0000	0.0217	-1.0000
		138600	6376465			

CAUSATIVE FACTOR	FACTOR CLASS	LANDSLIDE PIXEL	CLASS PIXEL	CP	PP	CF
SLOPE (degree)	0 - 7.81	9900	2462173	0.0040	0.0218	-0.8188
	7.81 - 17.43	40500	1634076	0.0248	0.0218	0.1233
	17.44 - 28.84	63000	1006603	0.0626	0.0218	0.6663
	28.85 - 41.46	22500	807769	0.0279	0.0218	0.2224
	41.47 - 76.61	2700	448659	0.0060	0.0218	-0.7283
		138600	6359280			

CAUSATIVE FACTOR	FACTOR CLASS	LANDSLIDE PIXEL	CLASS PIXEL	CP	PP	CF
CURVATURE	(-40.44) - (-3.33)	0	150618	0.0000	0.0217	-1.0000
	(-3.33) - (-0.77)	23400	978213	0.0239	0.0217	0.0934
	(-0.77) - 0.66	79200	4126175	0.0192	0.0217	-0.1192
	0.66 - 3.33	34200	976437	0.0350	0.0217	0.3878
	3.33 - 67.33	1800	145022	0.0124	0.0217	-0.4344
		138600	6376465			

CAUSATIVE FACTOR	FACTOR CLASS	LANDSLIDE PIXEL	CLASS PIXEL	CP	PP	CF
ASPECT	Flat (-1)	4500	425727	0.0106	0.0218	-0.5205
	North (0 - 22.5)	10800	494388	0.0218	0.0218	0.0024
	North-East (22.5 - 67.5)	8100	586242	0.0138	0.0218	-0.3712
	East (67.5 - 112.5)	17100	633343	0.0270	0.0218	0.1971
	South-East (112.5 - 157.5)	22500	733766	0.0307	0.0218	0.2957

	South (1575 - 202.5)	18900	783820	0.0241	0.0218	0.0983
	South-West (202.5 - 247.5)	18900	843659	0.0224	0.0218	0.0277
	West (247.5 - 292.5)	15300	716783	0.0213	0.0218	-0.0211
	North-West (292.5 - 337.5)	13500	599566	0.0225	0.0218	0.0328
	North (337.5 - 360)	9000	541986	0.0166	0.0218	-0.2421
		138600	6359280			

CAUSATIVE FACTOR	FACTOR CLASS	LANDSLIDE PIXEL	CLASS PIXEL	CP	PP	CF
SPI	(-13.82) - (-9.05)	2700	873396	0.0031	0.0218	-0.8608
	(-9.05) - (-4.94)	37800	1197227	0.0316	0.0218	0.3166
	(-4.94) - (-0.62)	27900	1606517	0.0174	0.0218	-0.2068
	(-0.62) - 2.19	57600	2035241	0.0283	0.0218	0.2350
	2.19 - 13.76	12600	646899	0.0195	0.0218	-0.1084
		138600	6359280			

CAUSATIVE FACTOR	FACTOR CLASS	LANDSLIDE PIXEL	CLASS PIXEL	CP	PP	CF
TWI	(-8.28) - (-1.82)	40500	2028813	0.0200	0.0218	-0.0858
	(-1.82) - 2.40	60300	1722053	0.0350	0.0218	0.3860
	2.40 - 5.22	28800	1643562	0.0175	0.0218	-0.1995
	5.22 - 9.22	8100	584932	0.0138	0.0218	-0.3698
	9.22 - 21.67	900	379920	0.0024	0.0218	-0.8934
		138600	6359280			

CAUSATIVE FACTOR	FACTOR CLASS	LANDSLIDE PIXEL	CLASS PIXEL	CP	PP	CF
DISTANCE TO RIVER (m)	0 - 8926.24	25200	1232644	0.0204	0.0216	-0.0544
	8926.24 - 17639.96	10800	1551405	0.0070	0.0216	-0.6824
	17639.97 - 26991.27	60300	1564846	0.0385	0.0216	0.4493
	26991.28 - 37617.75	31500	1279540	0.0246	0.0216	0.1255
	37617.76 - 54195.06	9900	747979	0.0132	0.0216	-0.3923
		137700	6376414			

CAUSATIVE FACTOR	FACTOR CLASS	LANDSLIDE PIXEL	CLASS PIXEL	CP	PP	CF
DISTANCE TO ROAD (m)	0 - 1210.12	108000	2790803	0.0387	0.0216	0.4517
	1210.12 - 2860.28	21600	1844719	0.0117	0.0216	-0.4632
	2860.28 - 5005.5	8100	1071799	0.0076	0.0216	-0.6550

	5005.5 - 8415.84	0	510132	0.0000	0.0216	-1.0000
	8415.84 - 14026.4	0	158961	0.0000	0.0216	-1.0000
		137700	6376414			

CAUSATIVE FACTOR	FACTOR CLASS	LANDSLIDE PIXEL	CLASS PIXEL	CP	PP	CF
DISTANCE TO LINEAMENT (m)	0 - 1324.67	88200	2116170	0.0417	0.0216	0.4925
	1324.68 - 2825.97	36000	1838453	0.0196	0.0216	-0.0951
	2825.97 - 4592.21	9900	1240895	0.0080	0.0216	-0.6356
	4592.22 - 6755.85	2700	805409	0.0034	0.0216	-0.8476
	6755.85 - 11259.76	900	375487	0.0024	0.0216	-0.8911
		137700	6376414			

CAUSATIVE FACTOR	FACTOR CLASS	LANDSLIDE PIXEL	CLASS PIXEL	CP	PP	CF
RAINFALL (mm)	669.53 - 743.01	0	421123	0.0000	0.0216	-1.0000
	743.02 - 816.48	0	461232	0.0000	0.0216	-1.0000
	816.49 - 889.96	9000	683791	0.0132	0.0216	-0.3957
	889.97 - 963.44	38700	956771	0.0404	0.0216	0.4764
	963.45 - 1036.9	90000	3853499	0.0234	0.0216	0.0770
		137700	6376416			

CAUSATIVE FACTOR	FACTOR CLASS	LANDSLIDE PIXEL	CLASS PIXEL	CP	PP	CF
LULC	WATER	0	252827	0.0000	0.0217	-1.0000
	TREES	77400	2987842	0.0259	0.0217	0.1645
	FLOODED VEGETATION	0	615	0.0000	0.0217	-1.0000
	CROPS	3600	569119	0.0063	0.0217	-0.7135
	BUILT AREA	45900	896908	0.0512	0.0217	0.5880
	BARE GROUND	0	216434	0.0000	0.0217	-1.0000
	SNOW/ ICE	0	332107	0.0000	0.0217	-1.0000
	CLOUDS	0	12	0.0000	0.0217	-1.0000
	RANGELAND	11700	1120288	0.0104	0.0217	-0.5250
		138600	6376152			

CAUSATIVE FACTOR	FACTOR CLASS	LANDSLIDE PIXEL	CLASS PIXEL	CP	PP	CF
GEOLOGY	QUATERNARY	2700	858197	0.0031	0.0217	-0.8580
	PLEISTOCENE	54900	2355382	0.0233	0.0217	0.0689
	PROTEROZOIC	8100	220615	0.0367	0.0217	0.4170

	PLIOCENE	33300	588364	0.0566	0.0217	0.6296
	MIOCENE	12600	586602	0.0215	0.0217	-0.0121
	PALAEOZOIC	900	456370	0.0020	0.0217	-0.9111
	NEOPROTEROZOIC	1800	1006662	0.0018	0.0217	-0.9194
	MIOCENE	21600	124277	0.1738	0.0217	0.8944
	PALAEOPROTEROZOIC	0	7913	0.0000	0.0217	-1.0000
	MIOCENE	2700	158597	0.0170	0.0217	-0.2205
	PALAEOZOIC	0	13492	0.0000	0.0217	-1.0000
		138600	6376471			

CAUSATIVE FACTOR	FACTOR CLASS	LANDSLIDE PIXEL	CLASS PIXEL	CP	PP	CF
LITHOLOGY	GRAVEL, PEBBLE, SAND, SILT AND CLAY	5400	248714	0.0217	0.0217	-0.0012
	DIAMICTITE, SHALE, SLATE, SANDSTONE, LIMESTONE	0	24227	0.0000	0.0217	-1.0000
	CARBONACEOUS SLATE, PHYLLITE, QUARTZITE	0	22410	0.0000	0.0217	-1.0000
	SILLIMANITE - KYANIE BEARING SCHIST, QUARTZITE	5400	137021	0.0394	0.0217	0.4584
	SLATE,PHYLLITE,QUARTZARENITE, LIMESTONE,METABASICS	1800	991305	0.0018	0.0217	-0.9181
	GREY PHYLLITE, SCHIST AND QUARTZITE	900	41856	0.0215	0.0217	-0.0110
	LEUCOCRATIC GRANITE, APLITE, QUARTZ VEINS.	900	453565	0.0020	0.0217	-0.9105
	BIOTITE GRANITE	0	12666	0.0000	0.0217	-1.0000
	PINK, GREY DOLOMITE, PHYLLITE, SHALE.	0	1361	0.0000	0.0217	-1.0000
	SHALE, SLATE, QUARTZITE, CHERTY DOLOMITE	0	603	0.0000	0.0217	-1.0000
	DOLOMITE, SPORADIC QUARTZITE.	0	2675	0.0000	0.0217	-1.0000
	STREAKY AND BANDED GNEISS.	900	11094	0.0811	0.0217	0.7483
	SALT GRIT, PURPLE GRIT,"LOKHAN"	0	1925	0.0000	0.0217	-1.0000
	THOLEIITIC BASALT MINOR QUARTZARENITE, SHALE	1800	17503	0.1028	0.0217	0.8062
	MICACEOUS SANDSTONE, PURPLE CLAY, MUDSTONE	17100	635219	0.0269	0.0217	0.1968
	GREY, PURPLE, RED SANDSTONE, SHALE, LIMESTONE	17100	164879	0.1037	0.0217	0.8080

	BROWN SANDSTONE, RED CLAY, PURPLE CHOCOLATE SHALE	5400	85631	0.0631	0.0217	0.6699
	GREY SAND, SILT AND CLAY	9900	384803	0.0257	0.0217	0.1586
	COARSE SANDSTONE, BOULDER CONGLOMERATE, CLAY & GRIT	40500	1767380	0.0229	0.0217	0.0526
	PINK, WHITE QUARTZITE, THIN BEDS OF RED SHALE.	0	435	0.0000	0.0217	-1.0000
	GREY MICACEOUS SANDSTONE, GRAVEL BEDS, SHALE, CLAY	28800	631037	0.0456	0.0217	0.5354
	QUARTZITE, SHALE, SLATE, A FEW BASIC FLOWS.	0	4450	0.0000	0.0217	-1.0000
	SCHIST AND QUARTZITE	0	35	0.0000	0.0217	-1.0000
	CARBONACEOUS SLATE, PHYLLITE, LIMESTONE, QUARTZITE	0	394	0.0000	0.0217	-1.0000
	PINK, GREY LIMESTONE, SPORADIC SHALE.	0	383	0.0000	0.0217	-1.0000
	DOLOMITE, BRICK RED SHALE.	0	166	0.0000	0.0217	-1.0000
	OXIDISED SILT-CLAY WITH KANKAR AND MICACEOUS SAND	1800	565584	0.0032	0.0217	-0.8563
	GREY MICACEOUS SAND, SILT AND CLAY	0	98681	0.0000	0.0217	-1.0000
	ILL SORTED BOULDER, COBBLE, PEBBLE IN SANDY MATRIX	900	70214	0.0128	0.0217	-0.4156
	GREEN, CARBONACEOUS SHALE, LIMESTONE, QUARTZITE	0	255	0.0000	0.0217	-1.0000
		138600	6376471			

CHAPTER 6

RESULT AND DISCUSSION

6.1. LANDSLIDE VULNERABILITY MAP

The landslide vulnerability map using FR, SE, IV, WoE, and certainty fact are plotted. Employing the natural break, the LSM was classified into 5 parts namely, very low, low, moderate, high, and very high for all the models. From the FR, it is apparent that 32 % of the total area lies in the high and very high class consisting of 85 % of all of the total landslide area, 30 % of the area lies in the moderate class consisting of 14 % landslide area, 38 % area lies in a low and very low class consisting of 1 % of the landslide area. From SE, it can be seen that 34 % of the total area is present in the high and very high classes consisting of 84 % of the total landslide area, 30 % of the area is present in the moderate class consisting of 15 % landslide area, 34 % area lies in a low and very low class consisting of 1 % of the landslide area. From the information value, it can be seen that 39 % of all of the area is present in the high and very high classes consisting of 87 % of all of the landslide area, 25 % of the area is present in the moderate class consisting of 11 % landslide area, 36 % area lies in a low and very low class consisting of 2 % of the landslide area. From the weight of evidence, it can be seen that 36 % of all of the area is present in the high and very high classes consisting of 91 % of the total landslide area, 24 % of the area is present in the moderate class consisting of 6 % landslide area, 40 % area is present in a low and very low class consisting of 2 % of the landslide area. From the CF, it can be seen that 45 % of the total area is present in the high and very high classes consisting of 95 % of the total landslide area, 23 % of the area is present in the moderate class consisting of 4 % landslide area, 32 % area is present in a low and very low class consisting of 0.5 % of the landslide area. The region-wide distribution of landslide and class area is shown in Table 6.1. and landslide-prone region-wide distribution of Kangra is shown in Fig. 6.1.

Table 6.1. Region-wide distribution of landslide and class area

	Landslide Susceptibility Class	Landslide Area	Landslide Area (%)	Class Area	Class Area (%)
FR	Very Low	0	0.00	1084233	17.05
	Low	900	0.65	1357935	21.35
	Moderate	19800	14.38	1865674	29.34
	High	42300	30.72	1429920	22.49
	Very High	74700	54.25	621518	9.77

	Landslide Susceptibility Class	Landslide Area	Landslide Area (%)	Class Area	Class Area (%)
SE	Very Low	0	0.00	1028819	16.18
	Low	900	0.65	1193855	18.77
	Moderate	20700	15.03	1937374	30.47
	High	48600	35.29	1496497	23.53
	Very High	67500	49.02	702735	11.05

	Landslide Susceptibility Class	Landslide Area	Landslide Area (%)	Class Area	Class Area (%)
IV	Very Low	900	0.65	996238	15.67
	Low	1800	1.31	1253351	19.71
	Moderate	14400	10.46	1585126	24.93
	High	54000	39.22	1794205	28.21
	Very High	66600	48.37	730360	11.48

	Landslide Susceptibility Class	Landslide Area	Landslide Area (%)	Class Area	Class Area (%)
WoE	Very Low	900	0.65	1213929	19.09
	Low	1800	1.31	1348306	21.20
	Moderate	9000	6.54	1529605	24.05
	High	42300	30.72	1650295	25.95
	Very High	83700	60.78	617145	9.70

	Landslide Susceptibility Class	Landslide Area	Landslide Area (%)	Class Area	Class Area (%)
CF	Very Low	0	0.00	889023	13.98
	Low	900	0.65	1160927	18.26
	Moderate	5400	3.92	1444144	22.71
	High	34200	24.84	1945041	30.59
	Very High	97200	70.59	920145	14.47

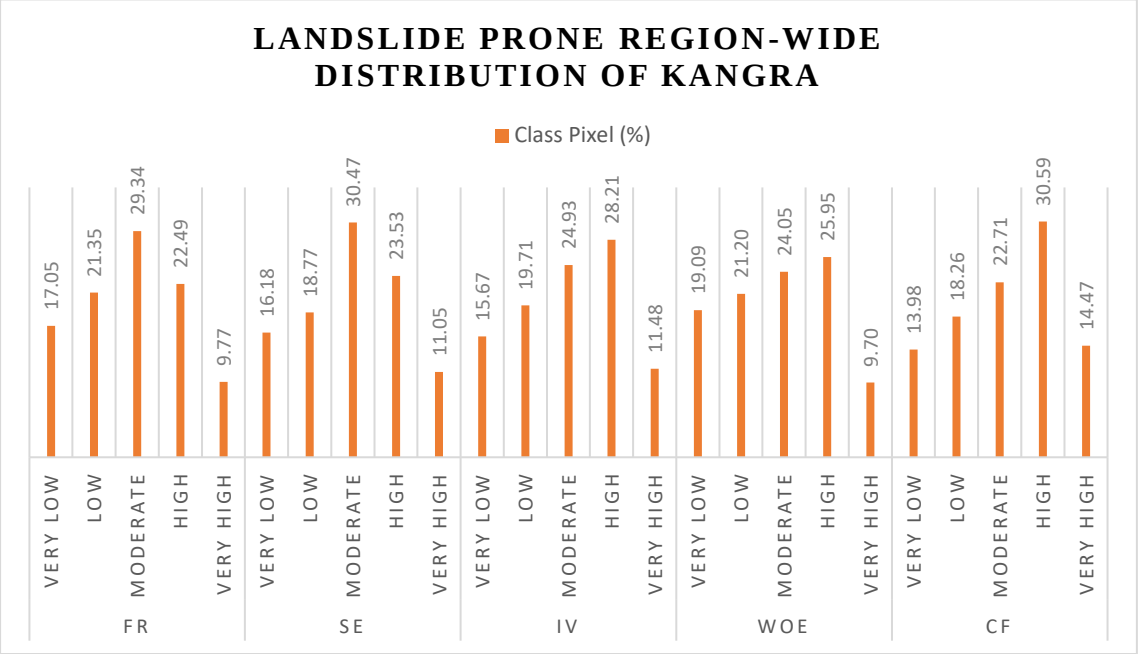

Fig. 6.1. Landslide prone region-wide distribution of Kangra

6.1.1. Frequency Ratio

The frequency ratio helps in determining the prediction rate of the activating factor which helps in knowing the exact triggering factor for the landslide occurrence. The higher value of the prediction rate represents the importance of that particular factor in the occurrence of a landslide. In our research, distance to roads got the highest prediction rate of 7.00, this may be because a lot of construction work is taking place by cutting the mountains. The prediction rate of rainfall is also 5.15 which plays a very important role in causing the landslide by weakening the soil strength. The bar chart showing the prediction rate of different factors is shown in Table 3. The study shows that there is a higher probability of occurrence of landslide in Kangra district when; elevation ranges between 728 m to 1700 m, slope ranges between 15 to 30 degrees, the curvature is between 0.66 to 3.33, SPI ranges between (-9.05) to (-4.94) and (-0.62) to 2.19, TWI ranges between (-1.82) to 2.40, distance to river range between 17,639 m to 37,617 m, distance to road ranges between 0 to 1,210 m, distance to lineaments ranges between 0 to 1,324 m, rainfall ranges between 890 mm to 1037 mm, land use for built areas, and geology. The prediction rate for all the

factors calculated using Frequency Ratio is shown in Fig. 6.2. and the vulnerability map is shown in Fig. 6.3.

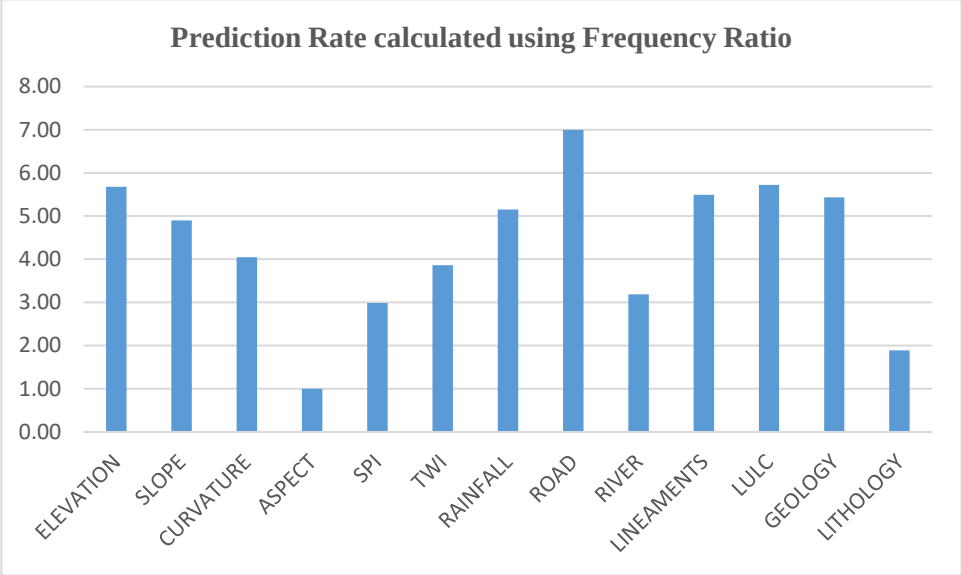

Fig. 6.2. Prediction rate using Frequency Ratio

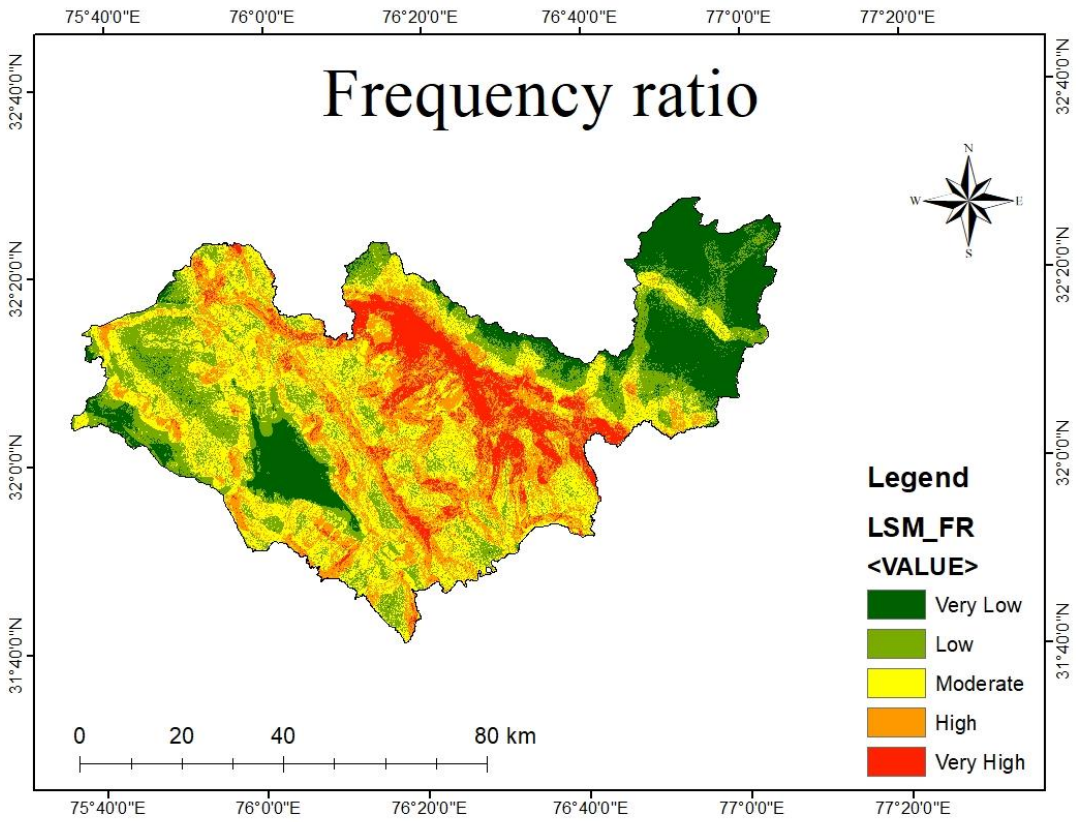

Fig. 6.3. Landslide Vulnerability Map for Frequency Ratio model

6.1.2. Shannon's Entropy

SE helps in arriving at the weights of the activating factors. From the findings of our study, the weights of land use land cover and distance to roads are highest having an approximate value of 0.14 with rainfall thereafter, geology, and elevation with a value of 0.11 approximately. The bar chart showing the weights calculated for all 13 activating factors is shown in Table 3. Numerically, it can be visualized as an extension of the frequency ratio model as the weights are calculated with the help of values of reduced factors. The weights for all the factors calculated using Shannon's Entropy are shown in Fig.6.4. and the vulnerability map is shown in Fig. 6.5.

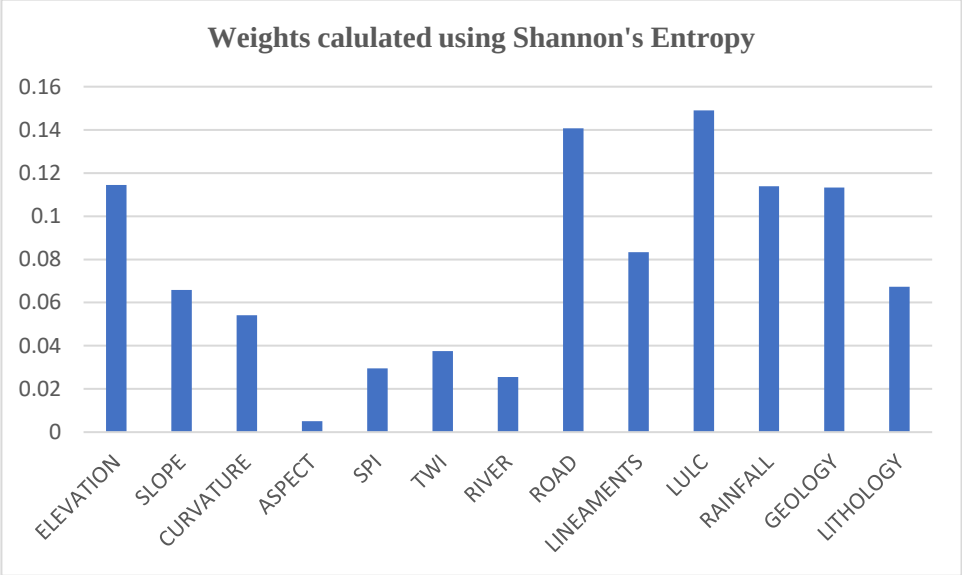

Fig. 6.4. Weights using Shannon's Entropy

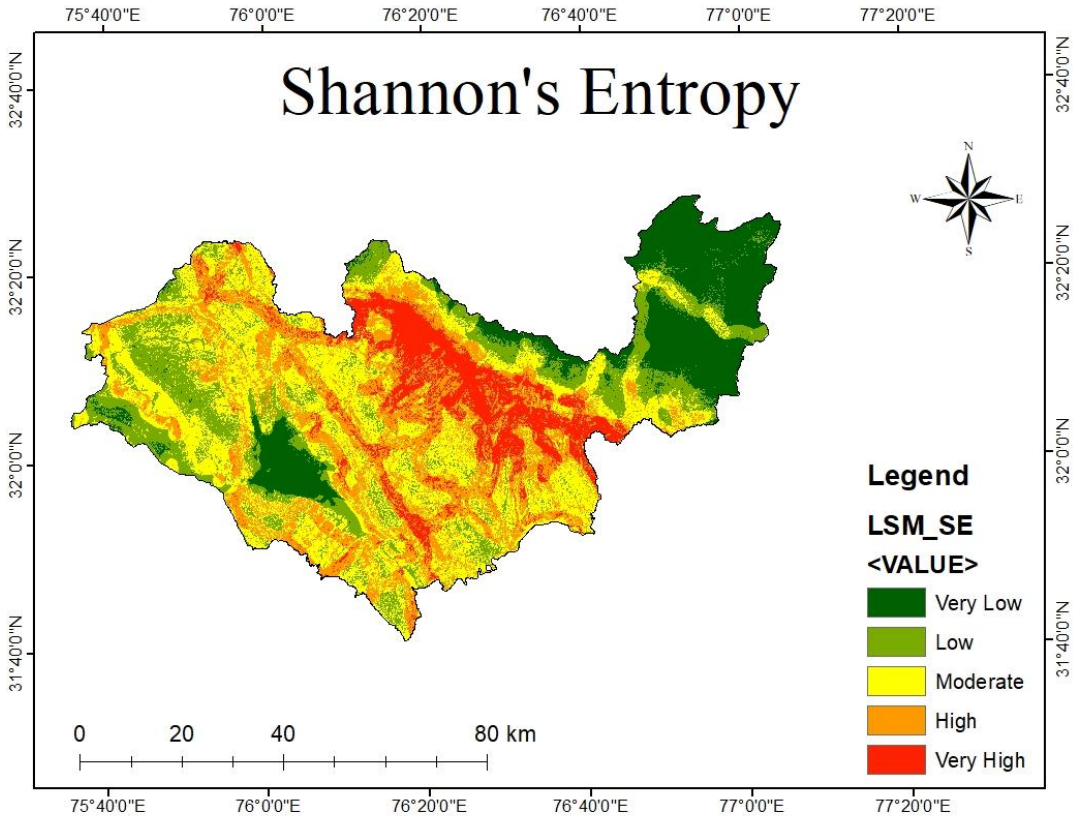

Fig. 6.5. Landslide Vulnerability Map for Shannon's Entropy model

6.1.3. Information Value

The IV helps in determining the likelihood of a landslide event. The positive value of IV represents a greater probability of the event of landslides whereas the negative value represents a lesser probability. The study shows that there is a higher probability of occurrence of landslide in Kangra district when; elevation ranges between 728 m to 1700 m, the slope ranges between 8 to 40 degrees, the curvature is between (-3.33) to (-0.77) and 0.66 to 3.33, SPI ranges between (-9.05) to (-4.94) and (-0.62) to 2.19, TWI ranges between (-1.82) to 2.40, distance to river range between 17,639 m to 37,617 m, distance to road ranges between 0 to 1,210 m, distance to lineaments ranges between 0 to 1,324 m, rainfall ranges between 890 mm to 1037 mm, land use for built areas, and geology. The vulnerability map created using information value is shown in Fig. 6.6.

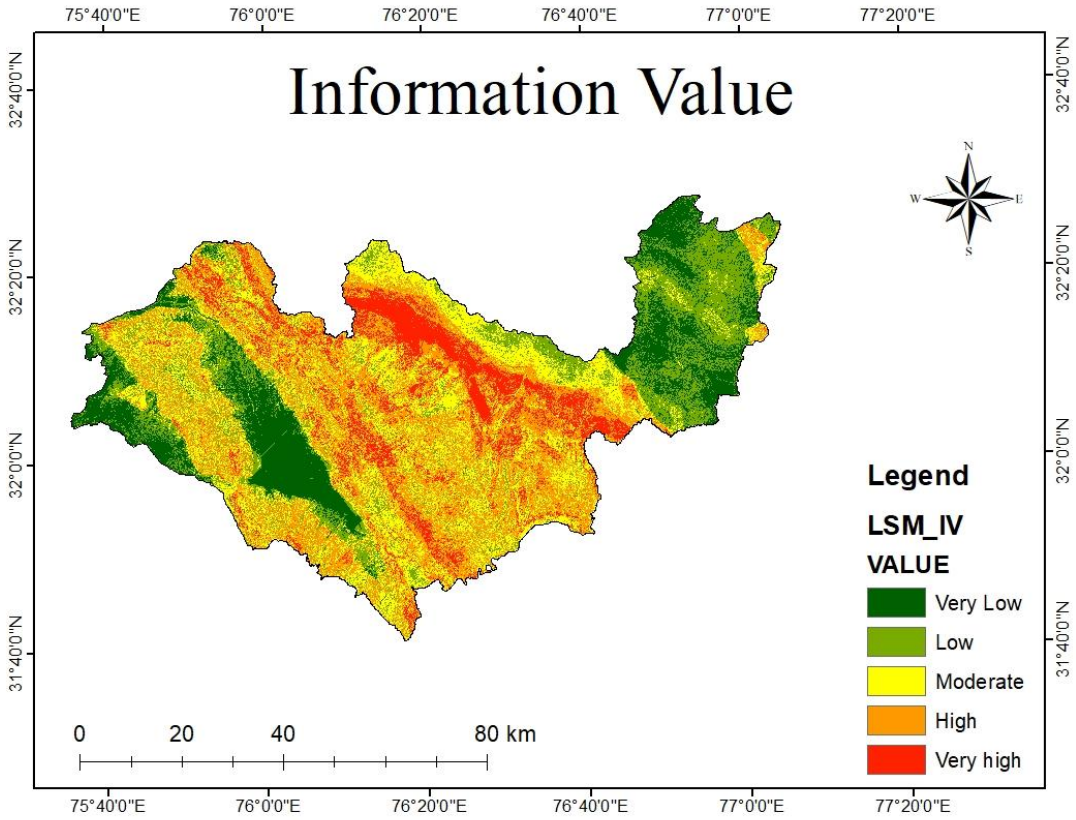

Fig. 6.6. Landslide Vulnerability Map for Information Value model

6.1.4. Weight of Evidence

The WoE helps in determining the likelihood of a landslide event by calculating the contrast value (C) for every class of all the factors. The negative value of C represents the lesser chances of landslide occurrence whereas the positive value represents high occurrence probability. The study shows that there is a higher probability of occurrence of landslide in Kangra district when; elevation ranges between 728 m to 1700 m, the slope ranges between 8 to 40 degrees, the curvature is between (-3.33) to (-0.77) and 0.66 to 3.33, SPI ranges between (-9.05) to (-4.94) and (-0.62) to 2.19, TWI ranges between (-1.82) to 2.40, distance to river range between 17,639 m to 37,617 m, distance to road ranges between 0 to 1,210 m, distance to lineaments ranges between 0 to 1,324 m, rainfall

ranges between 890 mm to 1037 mm, land use for built areas, and geology. The vulnerability map created with the help of the weight of evidence is shown in Fig. 6.7.

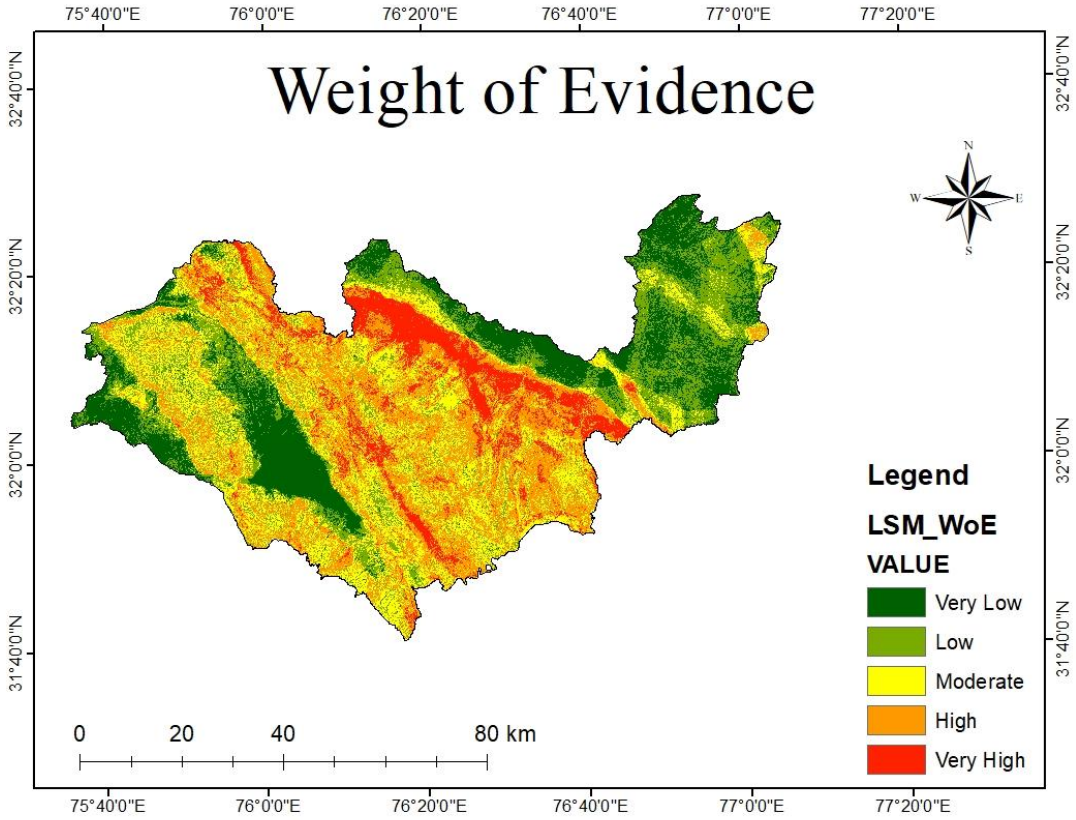

Fig. 6.7. Landslide Vulnerability Map for Weight of Evidence model

6.1.5. Certainty Factor

The certainty factor determines the conditional probability and prior probability which helps in the calculation of CF which decides the weightage of a certain class in a particular activating factor. The negative value indicates lower certainty in the event of landslides and a positive value indicates higher certainty in the occurrence of the landslide. The study shows that there is a higher probability of occurrence of landslide in Kangra district when; elevation ranges between 728 m to 1700 m, the slope ranges between 8 to 40 degrees, the curvature is between (-3.33) to (-0.77) and 0.66 to 3.33, SPI ranges between (-9.05) to (-4.94) and (-0.62) to 2.19, TWI ranges between (-1.82) to 2.40, distance to river range

between 17,639 m to 37,617 m, distance to road ranges between 0 to 1,210 m, distance to lineaments ranges between 0 to 1,324 m, rainfall ranges between 890 mm to 1037 mm, land use for built areas, and geology. The vulnerability map created with the certainty factor is displayed in Fig. 6.8.

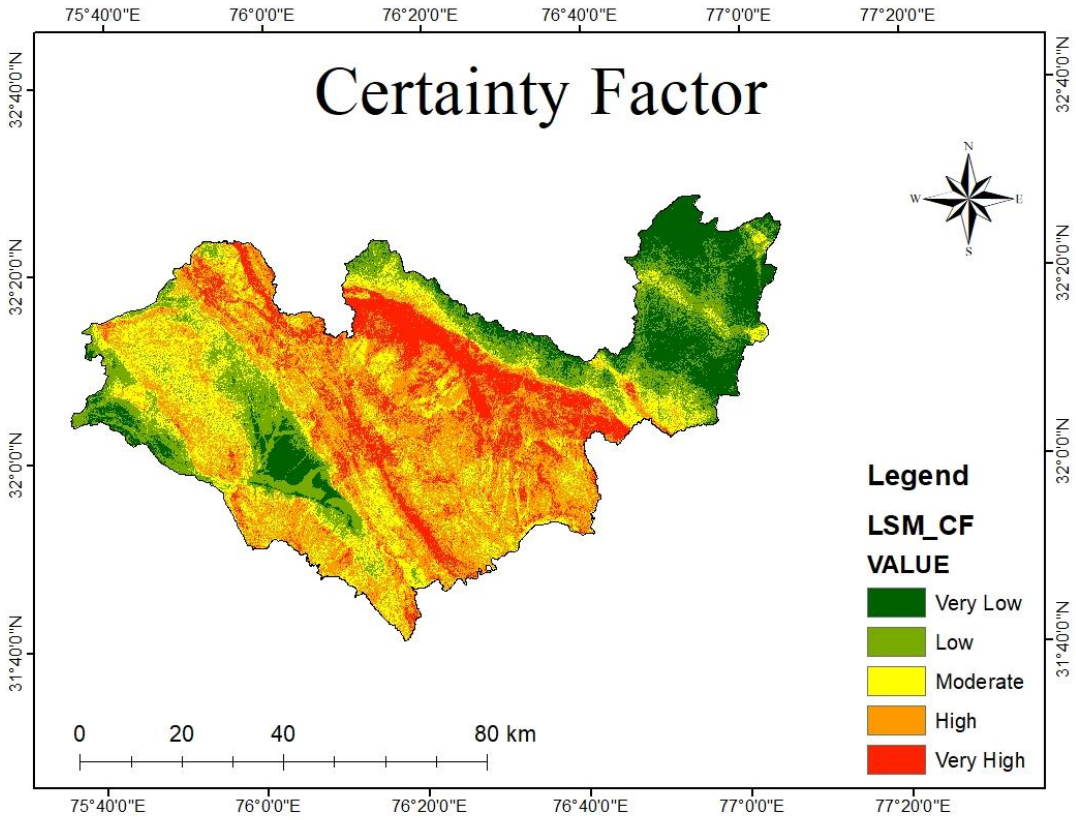

Fig. 6.8. Landslide Vulnerability Map for Certainty Factor model

6.2. MODEL VALIDATION

After the preparation of vulnerability maps, they need to be validated because, without validation, the model will be of no use. Out of 200 landslide points, 40 points (20%) have been kept for validating the model. There are many ways through which we can validate but, in our case, we are validating the model by calculating the AUC.

ROC is a performance indicator used to assess the quality of a binary classification model. The ROC curve is a graph that compares the TPR against the FPR at various categorization thresholds.

$$\text{True Positive Rate} = \frac{TP}{TP + FN} \qquad (6.1)$$

$$\text{False Positive Rate} = \frac{TN}{TN + FP} \qquad (6.2)$$

where,

TP and FP = True Positives and False Positives

TN and FN = True Negatives and False Negatives

TP and TN = pixels correctly classified as landslide and non-landslide

FP and FN = pixels incorrectly classified as landslide and non-landslide

Using the ROC tool, the SRC and PRC are plotted using training and testing landslide points simultaneously.

The area under the ROC curve, which spans from 0 to 1, is referred to as AUC. There exists a relationship between the AUC value and the performance of the mode as shown in Table 6.2.

Table 6.2. Relationship between AUC value and performance of the model

AUC Value	Performance
0.9 -1.0	Excellent
0.8 - 0.9	Very Good
0.7 – 0.8	Good
0.6 – 0.7	Average
0.5 - 0.6	Poor
Less than 0.5	Very Poor

This is the last part of the study. After carrying out the research work, validating the model is of utmost importance, without validation, it will be of no use. The validation is carried out using the AUC of ROC. The SRC and PRC are plotted for every model. The SRC comes out to be 0.863 and the PRC is 0.812 for the FR model. Similarly, the SRC and PRC for the SE model come out to be 0.844 and 0.0799 respectively. For the IV model, the SRC and PRC come out to be 0.83 and 0.755 respectively. For the WoE model, the SRC and PRC come out to be 0.88 and 0.794 respectively. For the CF model, the SRC and PRC come out to be 0.88 and 0.795 respectively. The SRC for all the models lies in the range of 0.8 – 0.9 which indicates the very good performance of the model and the

prediction rate is also close to 0.8 for all the models indicating very good performance. The success rate curves for all the models are shown in Fig. 6.9. whereas the prediction rate curves are shown in Fig. 6.10.

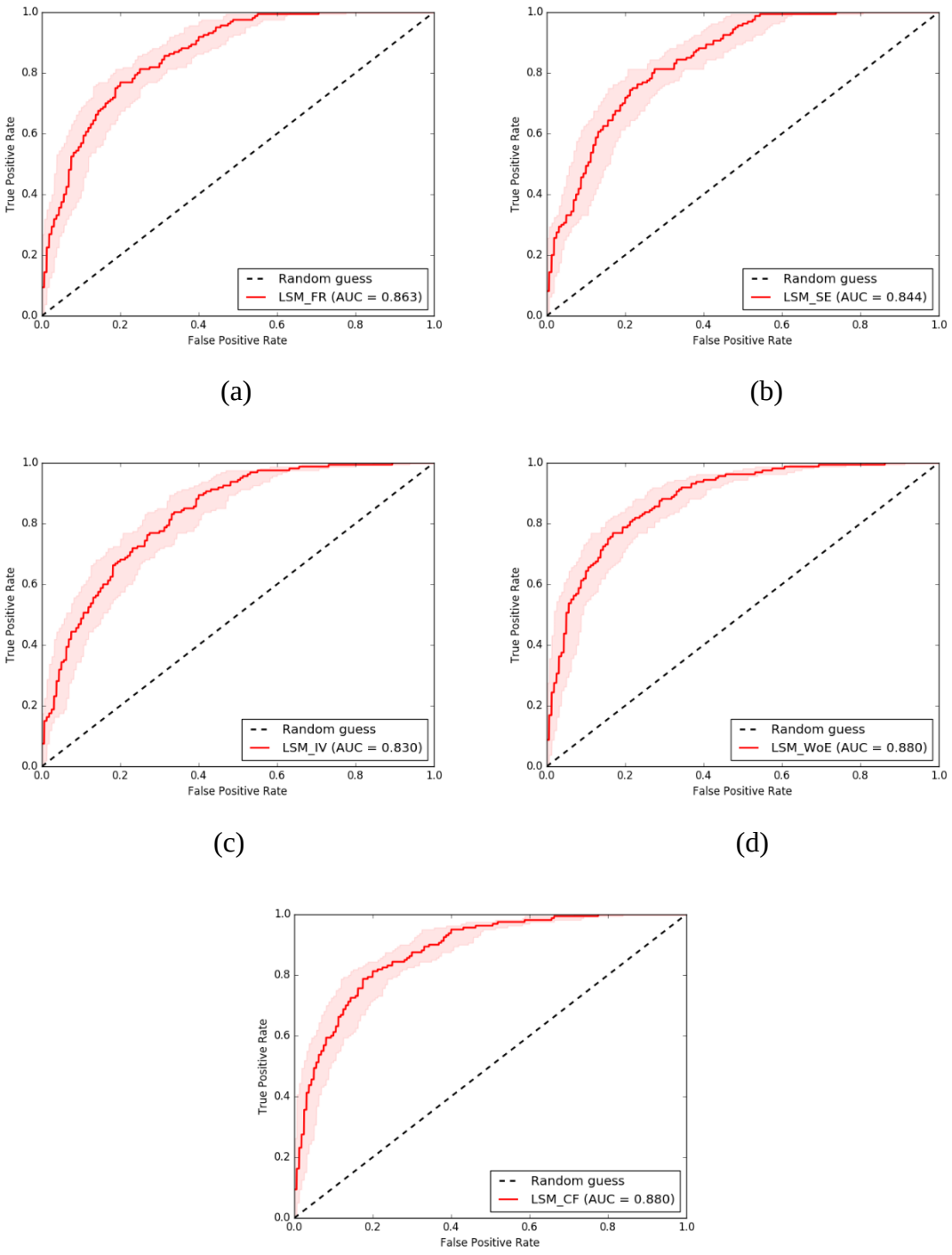

Fig. 6.9. Success Rate Curves for all the models

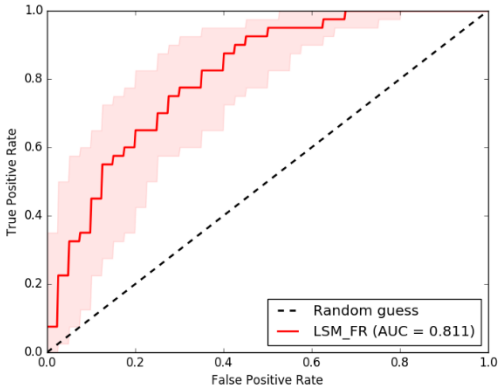

(a)

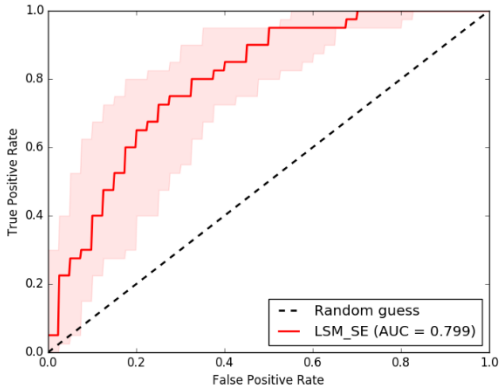

(b)

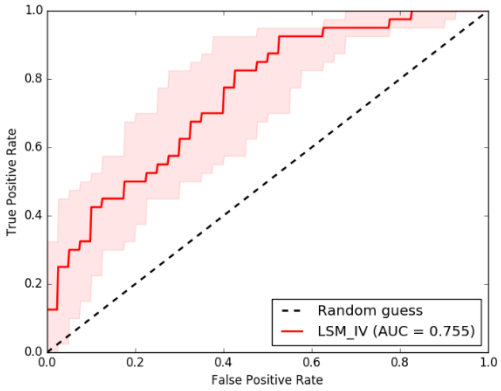

(c)

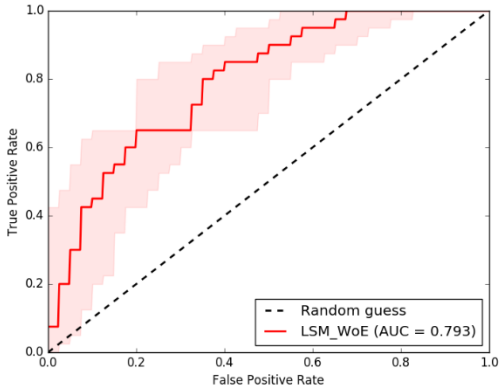

(d)

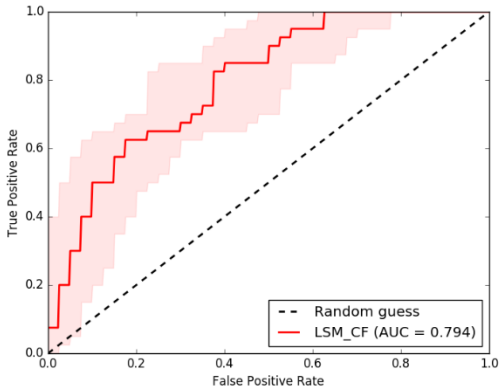

(e)

Fig. 6.10. Prediction Rate Curves for all the models

The success rate and prediction rate for all the models are tabulated as shown in Table 6.3.

Table 6.3. Success Rate and Prediction Rate for all the five models

MODELS	SUCCESS RATE	PREDICTION RATE
FR	0.863	0.811
SE	0.844	0.799
IV	0.83	0.755
WoE	0.88	0.794
CF	0.88	0.795

CHAPTER 7

CONCLUSION

7.1. CONCLUSION

Landslides are among the most deadly and costly natural disasters on the planet. They are a type of mass wasting, also known as landslips or mudslides, that may generate a wide range of ground motions. It causes the death of humans and other living beings alike, monetary loss, as well as environmental loss. FR, SE, IV, WoE, and CF models are used for the creation of a vulnerability map of Kangra, in HP, India. Kangra is a tourist spot of H.P. and is very prone to landslides. Thus, it is essential to create a vulnerability map of the area. Thematic maps of 13 factors are created for Kangra namely, elevation, slope, curvature, aspect, SPI, TWI, rainfall, distance to roads, rivers & lineaments, LULC, geology, and lithology. From the study, it can be concluded that 35 – 40% of the total area is present in the high and very high susceptible class, 25 – 30% of the area lies in the moderate class, 30 – 35 % of the area is present in low and very low susceptible class. It can also be concluded that proximity to roads, built area, rainfall, and geology are the triggering factor for most of the landslides that took place in the study area. The area under the curve of ROC is plotted for validating the results. The success rate comes out to be 0.863, 0.844, 0.83, 0.88, and 0.88 for the FR, SE, IV, WoE, and CF models respectively. The PRC comes out to be 0.812, 0.799, 0.755, 0.794, and 0.795 for the FR, SE, IV, WoE, and CF models respectively. The AUC values for success rate are near 0.9 which gives excellent performance and for prediction rate, it is near 0.8 which gives a very good performance. Although, WoE and CF model yields the maximum success rate whereas FR yields the maximum prediction rate. All 5 models give very good results and thus can be implemented in the Kangra district for mitigation purposes.

7.2. LIMITATIONS

The limitations observed during this research are:

- Only bivariate methods are used for the preparation of landslide vulnerability map while the landslides can have multivariate nature.
- LiDAR data may have been considerably better for creating a more precise picture of landslip susceptibility because they have a far greater resolution than satellite photography. However, a LiDAR survey is a very pricey operation that calls for highly qualified personnel and specialized tools.
- The study is totally data driven and data are collected from various sources whereas field investigation would have been possible but to carry out geotechnical field tests is very expensive.
- Other factors might have been considered such as NDVI (Normalized Difference Vegetation Index), Geomorphology, STI (Sediment Transportation Index), TRI (Topographic Roughness Index), etc.

7.3. FUTURE SCOPE

The government and higher authorities should keep this in mind so that any type of development project or market, cities, highways, tourist attractions, and so on, do not expand into the vulnerable sections of the basin in the future. These maps will be invaluable to planners and policymakers in developing strategies to limit and save the devastation caused by landslides.

REFERENCES

[1] A. Gadtaula and S. Dhakal, “Landslide susceptibility mapping using Weight of Evidence Method in Haku, Rasuwa District, Nepal,” *Journal of Nepal Geological Society*, vol. 58, pp. 163–171, Jun. 2019

[2] A. Rahaman, M. S. Venkatesan, and R. Ayyamperumal, “GIS-based landslide susceptibility mapping method and Shannon entropy model: a case study on Sakaleshapur Taluk, Western Ghats, Karnataka, India,” *Arabian Journal of Geosciences*, vol. 14, no. 20, Oct. 2021

[3] A. Wubalem and M. Meten, “Landslide susceptibility mapping using information value and logistic regression models in Goncha Siso Eneses area, northwestern Ethiopia,” *SN Applied Sciences*, vol. 2, no. 5, Apr. 2020

[4] C. E. Shannon, “A Mathematical Theory of Communication,” *Bell System Technical Journal*, vol. 27, no. 3, pp. 379–423, Jul. 1948

[5] D. Regmi, K.C. Devkota, K. Yoshida, B. Pradhan, H.R. Pourghasemi, T. Kumamoto and A. Akgun, “Application of frequency ratio, statistical index, and weights of evidence models and their comparison in landslide susceptibility mapping in Central Nepal Himalaya,” *Arabian Journal of Geosciences*, vol. 7, no. 2, pp. 725–742, Jan. 2013

[6] F. Guzzetti, A. C. Mondini, M. Cardinali, F. Fiorucci, M. Santangelo, and K.-T. Chang, “Landslide inventory maps: New tools for an old problem,” *Earth-Science Reviews*, vol. 112, no. 1–2, pp. 42–66, Apr. 2012

[7] F. Guzzetti, P. Reichenbach, M. Cardinali, M. Galli, and F. Ardizzone, “Probabilistic landslide hazard assessment at the basin scale,” *Geomorphology*, vol. 72, no. 1–4, pp. 272–299, Dec. 2005

[8] G. Demir, M. Aytekin, and A. Akgun, “Landslide susceptibility mapping by frequency ratio and logistic regression methods: an example from Niksar–Resadiye (Tokat, Turkey),” *Arabian Journal of Geosciences*, vol. 8, no. 3, pp. 1801–1812, Mar. 2014

[9] G. Du, Y. Zhang, Z. Yang, C. Guo, X. Yao, and D. Sun, “Landslide susceptibility mapping in the region of eastern Himalayan syntaxis, Tibetan Plateau, China: a comparison between analytical hierarchy process information value and logistic regression-information value methods,” *Bulletin of Engineering Geology and the Environment*, vol. 78, no. 6, pp. 4201–4215, Oct. 2018

[10] G. Hussain, Y. Singh, K. Singh, and G. M. Bhat, “Landslide susceptibility mapping along national highway-1 in Jammu and Kashmir State (India),” *Innovative Infrastructure Solutions*, vol. 4, no. 1, Nov. 2019

[11] H. Alsabhan, K. Singh, A. Sharma, S. Alam, D.D. Pandey, S. Rahman, A. Khursheed and F.M. Munshi, “Landslide susceptibility assessment in the Himalayan range based along Kasauli – Parwanoo road corridor using weight of evidence, information value, and frequency ratio,” *Journal of King Saud University - Science*, vol. 34, no. 2, p. 101759, Feb. 2022

[12] H. Shahabi, B. B. Ahmad, and S. Khezri, “Evaluation and comparison of bivariate and multivariate statistical methods for landslide susceptibility mapping (case study: Zab basin),” *Arabian Journal of Geosciences*, vol. 6, no. 10, pp. 3885–3907, Aug. 2012

[13] I. Das, A. Stein, N. Kerle, and V. K. Dadhwal, “Landslide susceptibility mapping along road corridors in the Indian Himalayas using Bayesian logistic regression models,” *Geomorphology*, vol. 179, pp. 116–125, Dec. 2012

[14] I. Yilmaz, “Landslide susceptibility mapping using frequency ratio, logistic regression, artificial neural networks and their comparison: A case study from Kat landslides (Tokat—Turkey),” *Computers & Geosciences*, vol. 35, no. 6, pp. 1125–1138, Jun. 2009

[15] J. Liu and Z. Duan, “Quantitative Assessment of Landslide Susceptibility Comparing Statistical Index, Index of Entropy, and Weights of Evidence in the Shangnan Area, China,” *Entropy*, vol. 20, no. 11, p. 868, Nov. 2018

[16] J. Varnes, “Slope movement types and processes,” *Transp. Res. Board Spec. Rep. 1978*, 176, 11-33, 1978.

[17] K. Batar and T. Watanabe, “Landslide Susceptibility Mapping and Assessment Using Geospatial Platforms and Weights of Evidence (WoE) Method in the Indian Himalayan Region: Recent Developments, Gaps, and Future Directions,” *ISPRS International Journal of Geo-Information*, vol. 10, no. 3, p. 114, Feb. 2021

[18] M. I. Sameen, R. Sarkar, B. Pradhan, D. Drukpa, A. M. Alamri, and H.-J. Park, “Landslide spatial modelling using unsupervised factor optimisation and regularised greedy forests,” *Computers & Geosciences*, vol. 134, p. 104336, Jan. 2020

[19] N. D. Dam et al., “Evaluation of Shannon Entropy and Weights of Evidence Models in Landslide Susceptibility Mapping for the Pithoragarh District of Uttarakhand State, India,” *Advances in Civil Engineering*, vol. 2022, pp. 1–16, Apr. 2022

[20] P. Gautam, T. Kubota, L. M. Sapkota, and Y. Shinohara, “Landslide susceptibility mapping with GIS in high mountain area of Nepal: a comparison of four methods,” *Environmental Earth Sciences*, vol. 80, no. 9, Apr. 2021

[21] P. Kayastha, “Landslide susceptibility mapping and factor effect analysis using frequency ratio in a catchment scale: a case study from Garuwa sub-basin, East Nepal,” *Arabian Journal of Geosciences*, vol. 8, no. 10, pp. 8601–8613, Feb. 2015

[22] P. Poudyal, C. Chang, H.-J. Oh, and S. Lee, “Landslide susceptibility maps comparing frequency ratio and artificial neural networks: a case study from the Nepal Himalaya,” *Environmental Earth Sciences*, vol. 61, no. 5, pp. 1049–1064, Feb. 2010

[23] Q. Wang, W. Li, Y. Wu, Y. Pei, M. Xing, and D. Yang, “A comparative study on the landslide susceptibility mapping using evidential belief function and weights of evidence models,” *Journal of Earth System Science*, vol. 125, no. 3, pp. 645–662, Apr. 2016

[24] R. Sarkar and K. Dorji, “Determination of the Probabilities of Landslide Events—A Case Study of Bhutan,” *Hydrology*, vol. 6, no. 2, p. 52, Jun. 2019

[25] S. Kumar and V. Gupta, “Evaluation of spatial probability of landslides using bivariate and multivariate approaches in the Goriganga valley, Kumaun Himalaya, India,” *Natural Hazards*, vol. 109, no. 3, pp. 2461–2488, Jul. 2021

[26] S. Mandal and S. Mondal, “Probabilistic Approaches and Landslide Susceptibility,” *Environmental Science and Engineering*, pp. 145–163, 2019

[27] S. Mondal and S. Mandal, “Landslide susceptibility mapping of Darjeeling Himalaya, India using index of entropy (IOE) model,” *Applied Geomatics*, vol. 11, no. 2, pp. 129–146, Nov. 2018

[28] S. Park, C. Choi, B. Kim, and J. Kim, “Landslide susceptibility mapping using frequency ratio, analytic hierarchy process, logistic regression, and artificial neural network methods at the Inje area, Korea,” *Environmental Earth Sciences*, vol. 68, no. 5, pp. 1443–1464, Aug. 2012

[29] S. Pasang and P. Kubíček, “Landslide Susceptibility Mapping Using Statistical Methods along the Asian Highway, Bhutan,” *Geosciences*, vol. 10, no. 11, p. 430, Oct. 2020

[30] S. Razavizadeh, K. Solaimani, M. Massironi, and A. Kavian, “Mapping landslide susceptibility with frequency ratio, statistical index, and weights of evidence models: a case study in northern Iran,” *Environmental Earth Sciences*, vol. 76, no. 14, Jul. 2017

[31] S. Sarkar, A. K. Roy, and T. R. Martha, “Landslide susceptibility assessment using Information Value Method in parts of the Darjeeling Himalayas,” *Journal of the Geological Society of India*, vol. 82, no. 4, pp. 351–362, Oct. 2013

[32] S. Sarkar, D. P. Kanungo, A. K. Patra, and P. Kumar, “GIS based spatial data analysis for landslide susceptibility mapping,” *Journal of Mountain Science*, vol. 5, no. 1, pp. 52–62, Mar. 2008

[33] S. Sharma and A. K. Mahajan, “A comparative assessment of information value, frequency ratio and analytical hierarchy process models for landslide susceptibility mapping of a Himalayan watershed, India,” *Bulletin of Engineering Geology and the Environment*, vol. 78, no. 4, pp. 2431–2448, Mar. 2018

[34] T. Mersha and M. Meten, “GIS-based landslide susceptibility mapping and assessment using bivariate statistical methods in Simada area, northwestern Ethiopia,” *Geoenvironmental Disasters*, vol. 7, no. 1, Jun. 2020

[35] W. Chen, H. Chai, X. Sun, Q. Wang, X. Ding, and H. Hong, “A GIS-based comparative study of frequency ratio, statistical index and weights-of-evidence models in landslide susceptibility mapping,” *Arabian Journal of Geosciences*, vol. 9, no. 3, Mar. 2016

[36] W. Chen, W. Li, H. Chai, E. Hou, X. Li, and X. Ding, “GIS-based landslide susceptibility mapping using analytical hierarchy process (AHP) and certainty factor (CF) models for the Baozhong region of Baoji City, China,” *Environmental Earth Sciences*, vol. 75, no. 1, Dec. 2015

[37] W. Chen, X. Ding, R. Zhao, and S. Shi, “Application of frequency ratio and weights of evidence models in landslide susceptibility mapping for the Shangzhou District of Shangluo City, China,” *Environmental Earth Sciences*, vol. 75, no. 1, Dec. 2015

[38] Y. Achour, A. Boumezbeur, R. Hadji, A. Chouabbi, V. Cavaleiro, and E. A. Bendaoud, “Landslide susceptibility mapping using analytic hierarchy process and information value methods along a highway road section in Constantine, Algeria,” *Arabian Journal of Geosciences*, vol. 10, no. 8, Apr. 2017

[39] Y. Cao, X. Wei, W. Fan, Y. Nan, W. Xiong, and S. Zhang, “Landslide susceptibility assessment using the Weight of Evidence method: A case study in Xunyang area, China,” *PLOS ONE*, vol. 16, no. 1, p. e0245668, Jan. 2021

[40] Z. Wu et al., “A comparative study on the landslide susceptibility mapping using logistic regression and statistical index models,” *Arabian Journal of Geosciences*, vol. 10, no. 8, Apr. 2017

LIST OF CONFERENCES

S. No.	Paper Title	Conference Name	Publication Partners	Current Status
1.	COMPARATIVE STUDY ON LANDSLIDE SUSCEPTIBILITY MAPPING USING TWO DIFFERENT STATISTICAL BIVARIATE METHODS FOR SOLAN, HIMACHAL PRADESH, INDIA	4th International Conference on Emerging Trends in Multi-Disciplinary Research (02-04 March 2023)	Scopus, UGC CARE, WEB OF SCIENCE	Accepted and Proceedings has been started ISBN: 978-93-5812-990-8
2.	GIS-BASED BIVARIATE STATISTICAL ANALYSIS USING FIVE DIFFERENT METHODS FOR LANDSLIDE VULNERABILITY MAPPING AND COMPARISON OF THEIR PERFORMANCE IN KANGRA, HIMACHAL PRADESH, INDIA	3rd International Conference on Engineering, Social-Sciences and Humanities (30-31 March 2023)	Scopus, UGC CARE, WEB OF SCIENCE	Accepted and under process

PAPER NAME

Anshu Kumar_2K21 GTE 06.pdf

AUTHOR

anshu kumar

WORD COUNT

15739 Words

CHARACTER COUNT

71325 Characters

PAGE COUNT

79 Pages

FILE SIZE

3.3MB

SUBMISSION DATE

May 24, 2023 1:04 PM GMT+5:30

REPORT DATE

May 24, 2023 1:05 PM GMT+5:30

13% Overall Similarity

The combined total of all matches, including overlapping sources, for each database.

- 7% Internet database
- 10% Publications database
- Crossref database
- Crossref Posted Content database
- 8% Submitted Works database